`

AN IMPROVED DIRECTION FINDING SYSTEM ANTENNA USING METHOD OF MOMENT APPROACH

By

OGONNA FRANCES ANAEBO (B. Eng)
REG NO: 20154944848

A PROJECT REPORT SUBMITTED TO THE POSTGRADUATE SCHOOL
FEDERAL UNIVERSITY OF TECHNOLOGY, OWERRI

IN PARTIAL FULFILLMENT OF THE REQUIREMENTS FOR THE AWARD OF MASTER OF ENGINEERING (M. ENG) DEGREE IN ELECTRICAL/ELECTRONIC ENGINEERING (COMMUNICATION ENGINEERING OPTION)

SCHOOL OF ENGINEERING AND ENGINEERING TECHNOLOGY

DECEMBER, 2019

CERTIFICATION

This is to certify that this work, "**An Improved Direction Finding System Antenna Using Method of Moment (MoM) Approach**," was carried out by **Ogonna Frances Anaebo (20154944848)** in partial fulfillment for the award of the degree of Master of Engineering (M. Eng) in Communication Engineering in the Department of Electrical and Electronic Engineering of the Federal University of Technology Owerri, Imo State.

ENGR. PROF. (MRS.) G. N. EZEH
(Supervisor)
DATE 21/9/21

ENGR. DR. N. CHUKWUCHEKWA
(Ag. H.O.D)
DATE 21/9/21

ENGR. PROF. J. C. EZEH
(Dean, S.E.E.T)
DATE 01/11/2021

PROF. C.C. EZE
Dean of Postgraduate School (PGS)
DATE

(External Examiner)
DATE 21/9/21

`

DEDICATION

This research work is dedicated to Almighty GOD, the author of all wisdom. I also dedicate it to all the lovers and sharers of positive knowledge.

`

ACKNOWLEDGEMENTS

I wish to acknowledge all the people that contributed in many ways to the success of this thesis.

I am most grateful to Engr. Prof. (Mrs.) G. N. Ezeh for accepting to supervise this work. All her advice and constructive criticisms are highly appreciated.

My thanks goes to the able head of my department, Dr. (Mrs.) I. E. Achumba for the excellent way she pilots the affairs of the department.

In a special way, I thank all the lecturers in Electrical/Electronic Engineering Department, FUTO. Engr. Prof. (Mrs) G.A Chukwudebe, Engr. Prof. E.N.C. Okafor, Engr. Prof. M. C. Ndinechi, Engr. Prof. F.K. Opara, Engr. Prof. D.O. Dike, Engr. Prof. F. I. Izuegbunam, Engr. Dr. L.O Uzoechi, Engr .Dr. C.K Agubor, Engr. Dr. C.C. Mbaocha, Engr. Dr. N. Chukwuchekwa, Engr. Dr. O. J. Onojo, Engr. Dr. O. C. Nosiri and Engr. Dr. M. Olubiwe.

My thanks also goes to my parents, Mr. and Mrs. G.M Anaebo for their financial assistance and encouragement.

My warmest regards and big thank you to my siblings, my colleagues in the class room, and so many other people too numerous to mention that contributed in various ways to the success of this work.

`

TABLE OF CONTENTS

`

`

CHAPTER FOUR: RESULTS AND DISCUSSIONS

CHAPTER FIVE: CONCLUSIONS AND RECOMMENDATIONS

`

LIST OF TABLES

`

LIST OF FIGURES

`

`

LIST OF PLATES

`

ABSTRACT

This study focuses on the Performance Improvement of a Direction Finding System Antenna Using Method of Moment (MoM) Approach. The work was developed to provide an approximate current distribution for a direction finding system antenna by employing the use of Method of Moment on an array of Yagi-uda antenna. The parameters of the experimental antenna were derived and analyzed using Magnetic Vector Potential (MVP) operator. The accurate current flowing through the radiating elements of the direction finding system was analyzed using combination of Method of Moment technique and Magnetic Vector Potential (MVP) operator. The antenna parameters were simulated using MatLab R2010a software tools. From the results obtained, the Average Poynting vector of the designed yagi antenna is 3.73 watt per square metre, and Radiation Intensity value of about 9.400 columns per kilogram. The simulation results also indicated an appreciable increase in directivity of 9.03dBi and enhanced directive gain compared to that of the equivalent log-periodic antenna of 6.5dBi, signifying 2.53dBi enhancement.

Keywords: Yagi Antenna, Moment Method, Wireless Communication, electromagnetic waves, wire Antennas, Ultra High Frequency (UHF), Magnetic Vector Potential.

`

CHAPTER ONE

INTRODUCTION

1.1 Background of the Study

The high spate of security attacks from fraudsters and indiscriminate use of communication frequencies by hoodlums have no doubt had a distressing effect on the country's economy. These necessitated the need for the detection of the direction and location of these fraudsters using a direction finding system. Development of a comparatively miniature but enhanced broadband direction finding system to be deployed with airborne or ground crafts is of concern in both military and civilian applications. The surreptitious tracking of these opponent fighters through their wireless communications is a main concern in the combat on terror both now and in the future time.

Since World War I, the ability to track the position of an enemy broadcaster has been so invaluable (Gladwin, 1997). It played a major role in World War II's Battle of the Atlantic. It is guesstimated that the UK's advanced "huff-duff" systems were accountable for 24% of all U-Boats sunk during the war (Rao, Singh and Singh, 2014). A number of diverse generations of Direction Finding (DF) systems have been deployed over time, following the development of novel electronics.

Early systems used mechanically rotated antennas that compared signal strengths in different directions, and numerous electronic versions of the same concept followed (Rao, *et al.,* 2014).Current systems often made use of phased array antennas to ensure swift beam forming for very accurate results. These are

`

usually incorporated into a wider electronic warfare suite. The systems employ the comparison of phase or doppler techniques which are usually simpler to automate. Modern pseudo-Doppler direction finding systems consist of a few miniature antennas fixed to a circular card, with all of the processing occurring in software (Abbosh, 2012).

According to (Lingel, Rhodes, Cordova, Hagen, Kvitky, and Menthe, 2008), for accurate performance of such surveillance and reconnaissance mission using direction finding system, directive and improved broadband antennas are required. Hence, the development of an antenna system that will proffer broad frequency ranges and ensure accurate direction finding capabilities is of great importance to these applications. Various antenna designers have contributed towards the advancement of this course via deployment of arrays of antennas of varying dimensions and configurations. These principles were helpful to the advancement of direction finding system but lacked precision required for detection of targets positions.

There is an apparent need for advanced analysis and design apparatus for forecasting the performance and optimizing the parameters of such antennas prior to costly prototype development and deployment (Douglas, 2014). In order to ensure high precision in antenna performance, there is great need to analyze the antenna parameters using an exact or approximate value of current flowing through the radiating elements. For decades, analysis of the vertical radiators and directional antennas arrays has been made by antenna designers using assumed current distribution. Also, for the sake of simplicity, uniformity and convenience, some antenna designers made use ofsinusoidal current distribution to simplify the mathematical integration of current along the length of each

`

antenna radiator in computing radiation characteristics (Alexander, 2012). However, as electromagnetic energy leaves the antenna, the forward and reflected currents are continuously attenuated as they travel the length of the antenna. Hence, the current vectors get increasingly smaller as they travel up and then down the antenna. When the forward and reflected current vectors are combined, they will not follow a sinusoidal curve (Alexander, 2012).

This research intends to improve the performance of the direction finding system by deploying Yagi-Uda array antenna and generating a close approximate current distribution and parameters for the antenna using the Method of Moment (MoM) approach. Method of Moment, also referred to as Moment Method, is one of the most prevailing numerical techniques used in the analysis of radiation and scattering problems in electromagnetic. An antenna being a radiator can be analyzed accurately by this technique. It was invented by Harrington (1968) and has been used by numerous authors (Asianuba, Nzeako and Sapre-Obi, 2014).

This technique demonstrated its flexibility and efficacy in resolving field problems. It is used to resolve problems based on electric or magnetic field integral equations essentially for analysis of wire antenna structures such as circular, linear, planar, arbitrarily oriented and elliptical structures. However, it is generally ineffective for the analysis of highly inhomogeneous media that has both frequency and time based modes of operation. Some of the numerous benefits of MoM include high efficiency, flexibility, accuracy, and sound theoretical formulation. The limitation of MoM is not due to the method

`

itself but relatively to the speed and storage capacity of the computing facility. (Asianuba *et al.,* 2014)

1.2 Problem Statement

The recent use of narrow band antennas, and the practice of using constant current and sinusoidal current sources in analyzing the performance of the antennas in direction finding system results in the development of a system that lacks precision. These result in high detection of false alarms and inability of the system to detect remote targets.

Also, it is observed that huge amount of money is usually spent in applying corrective measures trying to detect faults in direction finding system which ordinarily could have been averted if proper measures were taken before the antenna deployment.

In order to ensure high precision in the antenna performance, there is great need to analyze the antenna parameters using an exact or approximate value of current flowing through the radiating elements. This research study is focused on resolving this challenge of current accuracy by deploying Yagi array antenna and using method of moment in analyzing the accurate current flowing through the radiating elements of the direction finding system.

1.6 Objectives of the Study

The main objective of this research is to improve the performance of direction finding system antenna using method of moment (MoM) approach.

The specific objectives include:

`

i. To generate the current distribution for a direction finding system antenna using Method of Moment technique and Magnetic Vector Potential (MVP) operator.
ii. To design a typical direction finding system Yagi antenna with an improved directivity.
iii. To compute and analyze the parameters of Yagi antenna in a direction finding system using Magnetic Vector Potential (MVP) operator.

1.7 Justification of the Study

The outcome of this study will be of immense importance/guide to system designers towards designing and development of an efficient and cost effective direction finding system relative to the conventional system. The study will assist in anticipating antenna currents that are directly related to directional antenna parameters. Hence, it makes it possible to adjust the array to the desired parameters using antenna monitor parameters, provided that they accurately represent the antenna currents. This eliminates all the trial and error that is so much a part of the traditional array tune-up which in turn eliminates high detection of false alarms and inability of the system to detect remote targets.

More so, it will guide the system designers in predicting the base driving point impedances very accurately which allows for close design of the phasing and coupling system. Hence, it eliminates that guesswork, allowing the phasing and coupling system to be designed without all the "slack" for the unknowns. This is unlike in the existing systems in which the designing engineer will

`

have to ensure large variations in current distribution and load impedance because the exact operating parameters required to produce the required antenna pattern is unknown.

The outcome of this research will have an invaluable application on aircraft or ship for accurate navigational aid. This can be accomplished by measuring the direction (bearing) of two or more transmitters whose locations are already known. The measured directions from each transmitter are then plotted on a map, and the meeting point of the two plotted lines gives the location of the aircraft or ship carrying the DF. This technique is called triangulation.

Also, this research would have an important application in military operations as an accurate means for locating hostile transmitters and detecting the activities of potential enemies.

1.8 Scope of the Study

This thesis was limited to the improvement of direction finding system antenna using Method of Moment (MoM) approach. The parameters of the Yagi array antenna were analyzed at far field of the antenna.

The Method of Moment (MoM) was employed in connection with the Magnetic Vector Potential (MVP) technique to analyze the current, I flowing through the antenna elements. The antenna has single reflector, one active (driven) element and three parasitic directors.

The major design considerations considered in order to extend the bandwidth of the yagi array included: the Selection of the driven dipole for midband operations, increase of the length of reflector for low frequency operations, and

`

reduction of the length of directors for high frequency operations. It should be observed that the parasitic elements (directors) were used basically to augment gain at the upper and lower frequency limits of the reflecting element. MatLab R2010a object oriented programming language was used in the Antenna simulations.

`

CHAPTER TWO

LITERATURE REVIEW

2.1 Historical Perspective of the Antenna

An Antenna is any device that is capable of transmitting or receiving electromagnetic waves effectively with minimum loss of signals. It is a structure that is generally a metallic object, often a wire or group of wires, used to convert high frequency current into electromagnetic waves or to convert electromagnetic waves into high frequency current (Dhande, 2009).

The antenna or aerial is a means for radiating or receiving radio waves (IEEE Standard Definition of terms 145–1983). Antenna serves as an interface and a transforming device. As an interface it connects a transmitter or a receiver with the free space. As a transforming device it transforms the transmitter output impedance (50ohm/70ohm) into free space impedance ($\eta = 120\pi$ or 377ohm) (Warnick, 2014).

In any wireless communication system, the antenna plays a major role in determining the reliability and performance of the system. Its relevance is such that no electronic communication can take place without the existence of an antenna. Physically, an antenna is an arrangement of conductors that generates a radiating Electromagnetic (EM) field in response to an applied alternating voltage and the associate alternating electric current or can be placed in an electromagnetic field so that the field will induce an alternating current in the antenna and a voltage between its terminals (Staelin, 2011). Thus, an antenna is an essential part of Direction Finding Systems.

`

The idea of Radio Direction Finding (RDF) was born when Heinrich Hertz discovered the directional property of electromagnetic waves (Sinha, 2017). It was realized that antennas with directional properties boost field strength of the wanted signal and suppress that of the unwanted signals (side lobes) from other directions.

Direction finding or radio direction finding involves the determination of the direction from which a received signal was transmitted. By combining the direction information from two or more properly spaced receivers (or a single mobile receiver), the source of a transmitted signal could be located by way of triangulation. Hence, the use of radio direction finding is very essential in the navigation of ships and aircraft; it aids in location of illegal transmitters, for search and rescue operations, as well as for tracking wildlife.

2.2 Antenna Types and Applications

Antenna can be classified on the basis of:

i. Electromagnetic wave Transmission (Radiation) - Isotropic, Omni-directional, Directional, hemispherical antenna.

ii. Geometry – Wire Antenna, Aperture Antenna, Micro-strip Antennas and Array Antennas.

This section will briefly discuss some various forms of these antenna classifications in order to get a glance as to what the topic is all about.

`

2.2.1 Electromagnetic Wave Transmission (Radiation) Based Antenna

a. Isotropic Antenna

An isotropic antenna (radiator) is an ideal source that radiates equally in all directions.

Although it does not exist in practice, it provides a convenient isotropic reference with which to compare other antennas.. It is also called isotropic source or omnidirectional or simply unipole antenna.

An isotropic antenna is a hypothetical lossless antenna, with which the practical antennas are compared. Thus an isotropic antenna is used as reference antenna. Although sometimes, a half-wave dipole antenna is also used as reference antenna but these days the use of isotropic antenna as reference antenna is preferred (Dhande, 2009). Assume that a practical antenna is having a gain of 3dBi, it means that the gain of the practical antenna is three times more than that of an isotropic antenna when both antennas are connected with same source.

b. Omnidirectional Antenna

Omnidirectional antennas are those antennas which will cover equally well in azimuth direction and having some angle in elevation direction. Basically most of the wire antennas are having omnidirectional radiation pattern. Examples are Whip antenna, Dipole antennas, etc. The radiation patterns of omnidirectional antennas are shown in figure 2.1.

`

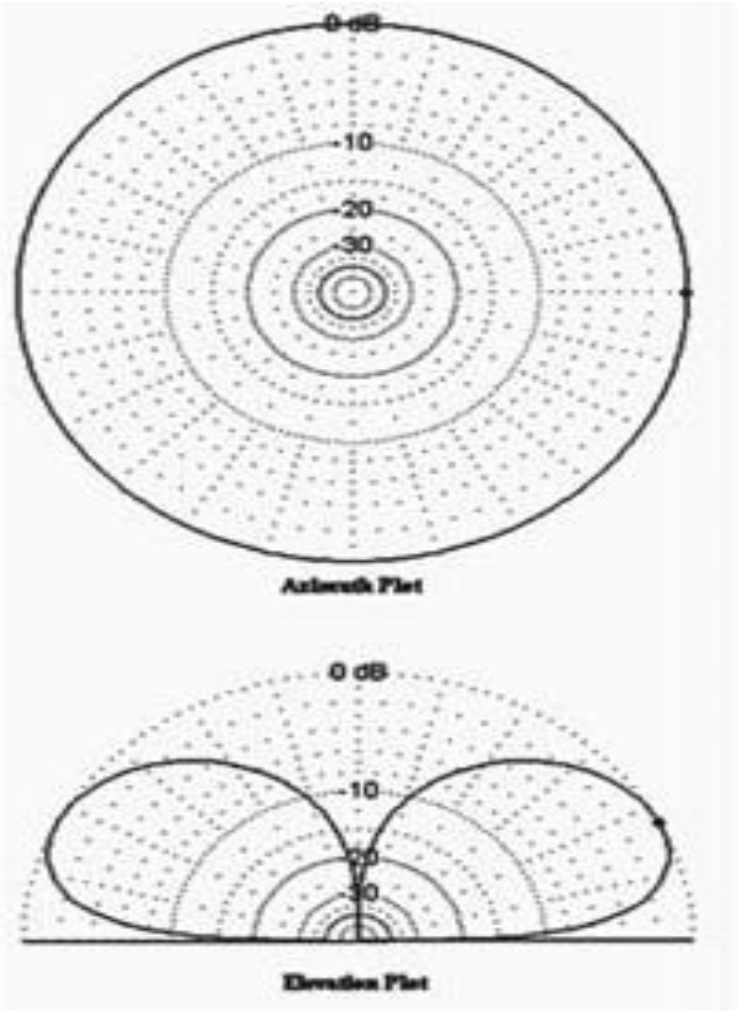

Figure 2.1: Omnidirectional Antenna (Balanis, 2005)

c. Directional Antenna

Antennas which directs its energy in one particular direction is said to be directional antennas. These antennas have very high gain and directivity to cover large wireless distance. Examples are parabolic reflector antenna, Yagi-Uda antenna, Log periodic antenna, etc. Radiation pattern of these antennas are shown in figure 2.2.

`

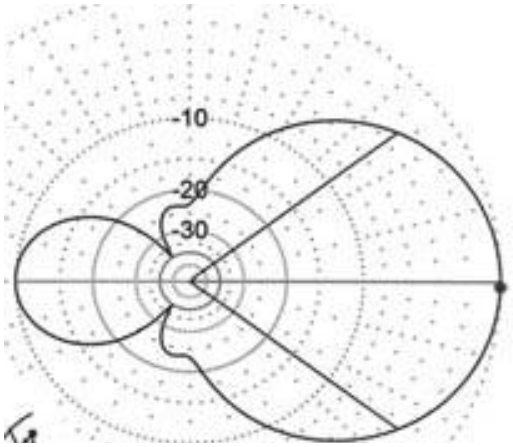

Figure 2.2: Directional Antenna radiation pattern (Balanis, 2005)

d. Hemispherical Antenna

Antenna whose radiation pattern will cover the one half of the hemisphere either upper or lower hemisphere is said to be antenna with Hemispherical Radiation pattern. Such types of antennas are implemented on aircraft body to cover the lower hemisphere for data link purpose. Examples are all Monopole antennas with large ground plane. The radiation pattern of these antennas is shown in figure 2.3.

`

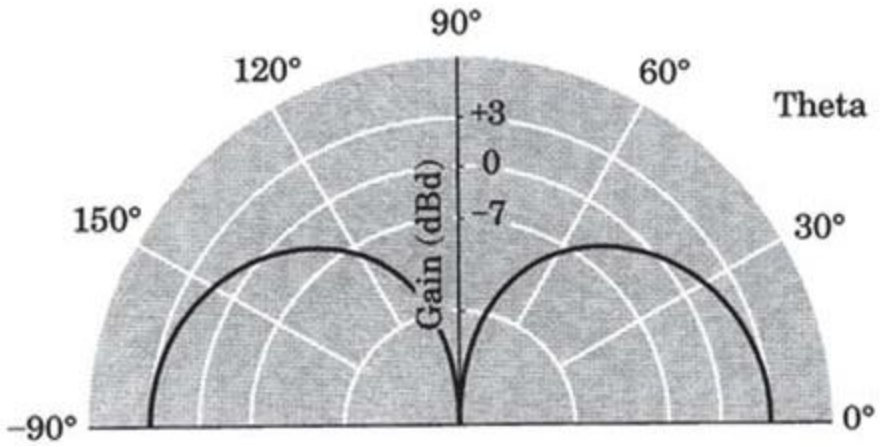

Figure 2.3: Upper hemispherical radiation pattern (Balanis, 2005)

2.2.4 Geometrical Based Antenna

a. Wire Antennas

As the name implies, these antennas are made of various forms of wire which shapes could be Dipole (straight wire), loop (rectangular, ellipse, square, circular etc), helix, array and so on. Figures 2.4 represent the diagram of various forms of the wire antenna.

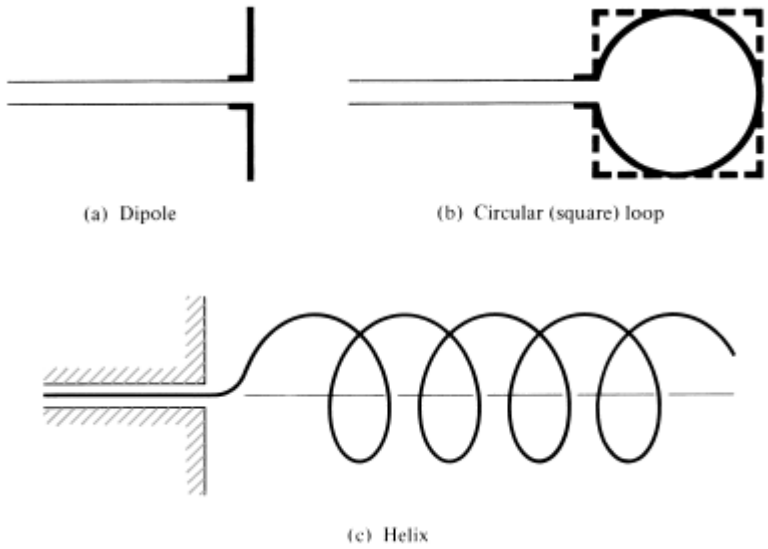

Figure 2.4: Wire antenna configurations (Kraus, 1997)

`

i. Dipole

The dipole derived its name from its two halves-one on each side of its centre. A dipole is a balanced antenna, meaning that the "poles" are symmetrical: They are equal in length and extend in opposite directions from the feed point. In its simplest form, a dipole is an antenna made of wire and fed at its centre as shown in the figure 2.5

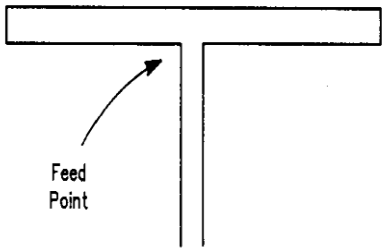

Figure 2.5: Block diagram of a folded wire dipole fed at its centre (Kraus, 1997)

To be resonant, a dipole must electrically be a half wavelength long at the operating frequency. A dipole resonance occurs at the length at which its impedance has no reactance, only resistance at a given frequency. The lowest frequency at which a dipole is resonant is known as its *fundamental resonance.* A dipole works best at and above its fundamental-resonant frequency. For almost any kind of MF/HF operation, dipoles are easy to build and install, and they give good results when put up at any reasonable height (Healy, 1991).

`

Dipoles operate at Medium Frequency, 300 - 3000KHz. They find applications in AM broadcasting, maritime radio, coast guard communication, direction finding etc. They also operate at Super High Frequency (SHF), applicable in Air bone RADAR, satellite communication, microwave links etc.

ii. Loop

A loop antenna is composed of a single loop of wire, greater than a half wavelength long. The loop does not have to be any particular shape. Loop antenna can have various shapes such as circular, triangular, rectangular, square, elliptical, etc. (Cicchetti *et al.,* 2017). In putting up a loop, it can be vertically oriented or horizontally oriented. Vertically oriented loops may be erected with one or between 2 supports, while horizontally oriented loop will require at least 3supports. Figure 2.6 shows the orientation of the loops.

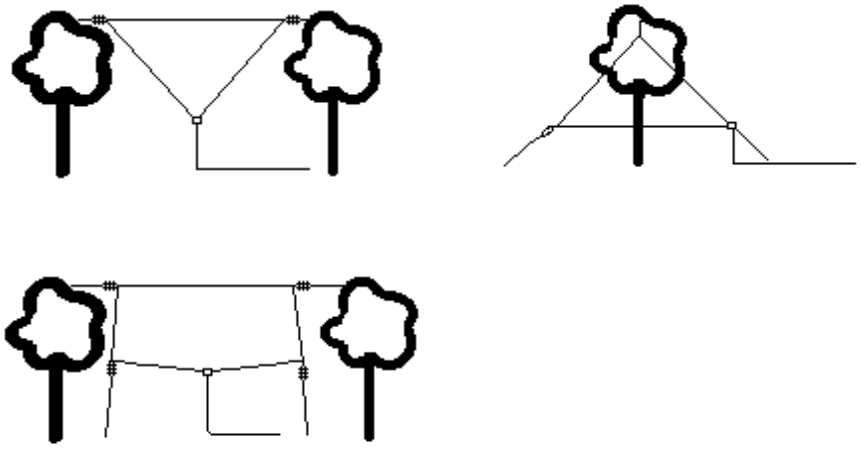

Figure 2.6: A loop antenna with its orientations (Kraus, 1997)

`

Loop antennas posses the following Characteristics:

a. Electrical length - the overall length of the dipole in wavelengths at the frequency of interest.
b. Directivity - the ratio of the maximum radiation of an antenna to the maximum radiation of a reference antenna. It is often measured in dBi, dB above an isotropic (non-directional) radiator.
c. Self Impedance - the impedance at the antenna's feed point (not the feed point in the shack).
d. Radiation Resistance - a fictitious resistance that represents power flowing out of the antenna
e. Radiation Pattern - the intensity of the radiated RF as a function of direction.

Loop antennas are mainly used at frequencies above 3.5 MHz where their size is manageable. They can be viewed as a folded dipole deformed into an open shape. This shape can be a circle, triangle, square, or rectangle, or in fact any polygon. The maximum radiation is at right angles to the plane of the loop. At the lower frequencies the physically large loop would be "laying down", that is, supported above the ground by several masts. The main beam is upwards. Above 10 MHz, the loop is more frequently "standing up", that is in the vertical plane, to direct energy towards the horizon. The loop may be rotatable. Compared to a dipole or folded dipole, it transmits slightly less toward the sky or ground, giving it about 1.5 dB higher gain in the two favoured horizontal directions.

`

iii. Helical or Helix Antenna

Helical or Helix Antenna is a wire antenna in which the conducting wire is wound in helical shape and connected to the ground plane with a feeder line. According to Rahim (2015), the Helix Antenna is a hybrid of two radiating elements, the dipole and loop antenna. A Helix becomes a linear antenna when its diameter approaches zero or pitch angle (α) goes to 90^0. On the other hand, a Helix of fixed diameter can be seen as a loop antenna when the spacing between the turns vanishes ($\alpha=0^0$). It is a specialized form of antenna, very useful in practical applications providing circularly polarized waves. A Helix Antenna is represented in plate 2.1.

Plate 2.1: Helix antenna (Balanis, 2005)

These antennas have been known for quite a while. Due to the reason of practical emission and easy to use, such antennas are extensively in practice from many years. In addition to that, these antennas are widely used in getting microwaves from very high frequency (VHF) and Utra High Frequency (UHF)

`

due to their properties is extremely extraordinary and exceptional. Its frequency of operation ranges from 30-300MHz. Helical antenna finds applications in satellite communication, Television, FM broadcast, Air traffic control, Navigational aids, Surveillance RADAR etc. The 50 Ohm coaxial link fed the geometry of this kind of antenna model design. It comprises of one empty dielectric chamber with relative permittivity 2.1 and distance across 61.33mm (Khan *et al*., 2016).

iv. Aperture Antennas

This is the type of antennas mainly used for aircraft and spacecraft applications. They can be very conveniently flush-mounted on the skin of the aircraft or spacecraft. These antennas are covered with dielectric materials to protect them from harmful environmental conditions. A typical example of this type of antenna is the waveguide aperture antennas. This is shown in Figure 2.7

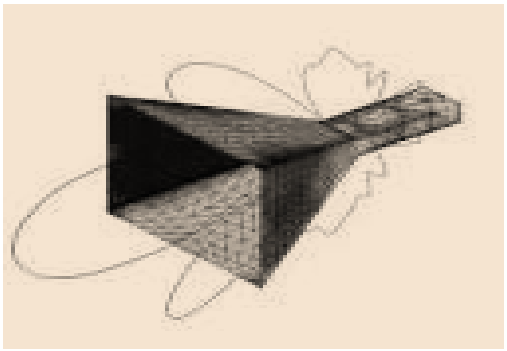

Figure 2.7: Waveguide aperture antenna (Balanis, 2005)

v. Micro-strip Antennas

`

These are very simple and low cost type of antennas. They consist of circular, triangular, or other forms of configuration of patches on a grounded substrate. These antennas find applications on high-performance aircrafts, spacecrafts, satellites, cars, and even handheld electronic devices like smart phone. Microstrip antennas are in the frequency range of 3-30GHz. Figure 2.8 show the diagrams of rectangular and circular patches.

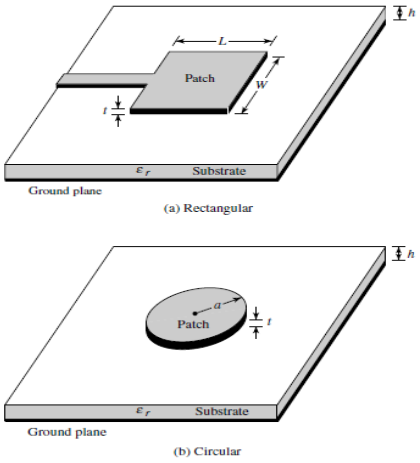

Figure 2.8: Rectangular and circular patches of a micro-strip antenna (Balanis, 2005)

vi. Array Antennas

An array involves combination of two or more radiating elements in an electrical and geometrical arrangement in order to achieve an intended radiation characteristics (Shi, 2014). An important characteristic of an array is the change of its radiation pattern in response to different excitations of its antenna elements. Unlike a single antenna whose radiation pattern is fixed, an antenna array's radiation pattern, called *the array pattern*, can be changed upon exciting

`

its elements with different currents (both current magnitudes and current phases). This gives a freedom to choose (or design) a certain desired array pattern from an array, without changing its physical dimensions. Furthermore, by manipulating the received signals from the individual antenna elements in different ways, it can achieve many signal processing functions such as spatial filtering, interference suppression, gain enhancement, target tracking, etc.

2.2.3 Antenna Applications

The most fundamental parts of any wireless communication framework is the antenna. It builds the connections between the free space and transmitter or free space and the receiver. Antennas converts RF signal or electrical signal into electromagnetic or wave signal (Xie, 2014). It receives electromagnetic signal and converts it into electrical signal. Functionally, antennas are devices use to send information in form of electromagnetic signal, to communicate wireless or unguided way. The radiation resistance of an antenna affects its efficiency. If the radiation resistance is high, the efficiency of that antenna will be high. Antennas are useful mode of communication in different fields; antennas are used to communicate in form of audio, video, graphics etc. as they are important in communication. Antennas are developed time to time according to the need; they are designed for different application of different materials, structures for better communication (Zhang *et al*., 2017). They are designed for radio, television, satellite, broadcasting, cellular system communications etc. Different systems have different kinds of antennas employed to them. In some systems, directional properties of the antennas are designed around by operational characteristics of the system.

`

For horn antennas, they are extensively used at microwave frequencies, ranging from 3-30GHz when the power gain needed is moderate. They find applications in Air bone RADAR, Microwave Links, experimental etc. For high power gains other antennas like lines or parabolic reflectors are preferred rather than horn antennas.

2.3 Antenna Parameters

In order to describe the performance of an antenna, it is necessary to interrelate it with various parameter characteristics. They include:

i. Electric and Magnetic fields (E & H Fields)
ii. Radiation power density
iii. Radiation Pattern
iv. Radiation Intensity
v. Radiated Power
vi. Radiation Resistance
vii. Antenna Impedance
viii. Directivity
ix. Effective Area

i. Electric and Magnetic fields (E & H Fields):

Electric magnetic fields (EMFs) are produced both naturally and as a result of human activity. The earth has both a magnetic field, produced by currents deep inside the molten core of the planet and an electric field, produced by electrical activity in the atmosphere, such as thunderstorm.

`

Electric fields are produced by voltage. Voltage is the pressure behind the flow of electricity. It can be likened to the pressure of water in a hose. Electricity at homes is at voltage of 230 volts (230 V), but outside homes it is distributed at higher voltages, from 11,000 volts (11 KV) up to 400,000 volts (400 KV). Generally, the higher the voltage, the higher the electric field. Electric fields are measured in volts per metre (V/m).

Magnetic fields are produced by current, which is the flow of electricity. Current, which is measured in amperes or amps, can be likened to the flow of water in a hose when the nozzle is open. Generally, the higher the current, the higher the magnetic field. Magnetic fields are measured in microtesla (μT).

One difference between electric and magnetic fields is that electric fields are very easily screened-by buildings, hedges, fences and trees. So inside a house will be very little electric field from a power line outside. By contrast, magnetic fields pass readily through most buildings.

Another difference is that a mains appliance such as a radio or lamp does not have to be operating to produce an electric field as long as it is plugged into a mains supply, it will produce an electric field. However, it produces a magnetic field only when it is turned on and drawing a current.

Whenever electricity is used there will also be electric and magnetic fields (EMFs), hence EMFs is inevitable (Ena, 2012).

Electric and Magnetic fields are generated by electric current density source **J** and magnetic current density source **M** respectively.

ii. Radiation Power Density:

`

According to Neelakanta and Chatterjee (2003), radiation power density expresses the power associated with an electromagnetic wave. It is the instantaneous poynting vector defined as

$$\mathbf{W} = (\boldsymbol{E} \times \boldsymbol{H}) \quad (2.1)$$

Where;

W = instantaneous poynting vector (W/M^2)

E = instantaneous electric field intensity (V/M)

H = instantaneous magnetic field intensity (A/M)

It is more suitable to find the average power density for applications concerning time varying fields. Hence, the time average poynting vector (average power density) can be written as; (Kraus and Marhefka, 2001)

$$\mathbf{P_{av}} = \tfrac{1}{2} (\boldsymbol{E} \times \boldsymbol{H}^{*}) \quad (2.2)$$

The average power density is obtained by integrating the instantaneous poynting vector over one period and dividing by the period. For applications of time-varying fields, it is desirable to find the average power density. For time-harmonic variations of the form $e^{j\omega t}$, the complex fields ***E*** and ***H*** are defined which are related to their instantaneous counterparts **E** and **H** by (Neelakanta and Chatterjee, 2003) as

$$\mathbf{E}(x, y, z; t) = \text{Re}\,[\boldsymbol{E}(x, y, z)\, e^{j\omega t}] \quad (2.3)$$

$$\mathbf{H}(x, y, z; t) = \text{Re}\,[\boldsymbol{H}(x, y, z)\, e^{j\omega t}] \quad (2.4)$$

Hence, the average power density (average poynting vector) can be written as:

$$\boldsymbol{W}\text{av} = \tfrac{1}{2}\,\text{Re}\,[\boldsymbol{E} \times \boldsymbol{H}^{*}]\ (W/m^2). \quad (2.5)$$

iii. Radiation pattern:

`

An antenna radiation pattern or antenna pattern is defined as a mathematical function or a graphical representation of the radiation properties of the antenna as a function of space coordinates (Ranga Rodrigo, 2010). It is often determined in the far-field region. Antenna radiation properties include radiation intensity, radiation resistance, directivity, and polarization among others. The plot of the magnitude of the electric and magnetic field as a function of the angular space gives the field pattern while the plot of the square of the magnitude of the electric and magnetic field as a function of the angular space produces the power pattern (Balanis, 2005).

iv. Radiation Intensity:

This is the power radiated from an antenna in a given direction per unit beam solid angle. The beam solid angle or beam area (Ω_A) of an antenna is defined as the integral of the normalized power pattern over a unit sphere. Radiation Intensity is expressed in watts per steradian (W/sr) and simply obtained by multiplying the time average poynting vector by the square of the distance. Written as:

$$\mathbf{U = r^2 P_{av}} \qquad (2.6)$$

v. Radiated Power:

A measure of how much power radiated by an antenna when the antenna is connected to an actual radio or transmitter is the Total Radiated Power (Balanis, 2005). Total radiated power is an active measurement, in that a powered transmitter is used to transmit through the antenna. The total received power is

`

calculated and summed up over all possible angles, hence it is spherical or 3D measurement and the result is the Total Radiated Power (TRP). It is closely related to the efficiency of the antenna, and is in fact tied to the definition of efficiency. In Figure 2.9, TRP is the output power, $\mathbf{P_{out}}$. Antenna efficiency $\boldsymbol{\eta_{antenna}}$, is the ratio of output power, $\mathbf{P_{out}}$ to input power, $\mathbf{P_{in}}$. TRP is expressed in terms of power: Watts (W), milliwatts (mW), or logarithmic terms for W and mW (dBW and dBm). Antenna efficiency is expressed either in percentage or dB.

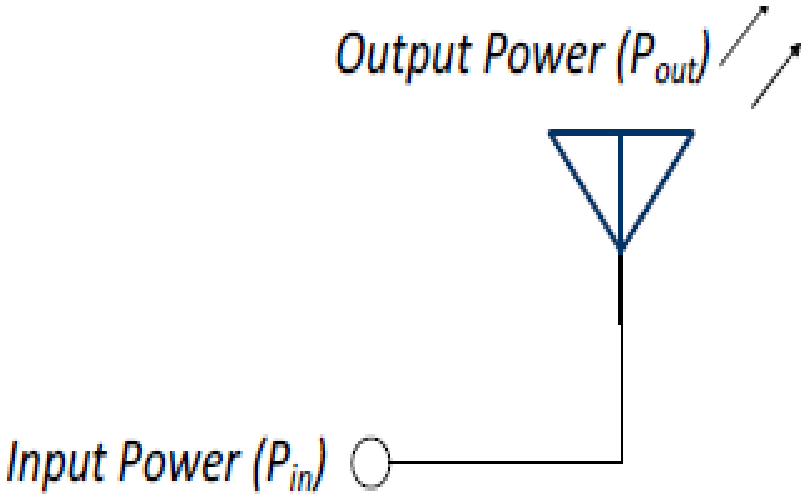

Figure 2.9: Input/Output Radiated power

$$\boldsymbol{\eta_{antenna}} = \frac{\mathbf{Pout}}{\mathbf{Pin}} = \frac{\mathbf{TRP}}{\mathbf{Pin}} \qquad (2.7)$$

vi. Radiation Resistance:

`

This is the point that the value of a hypothetic resistor will dissipate a power equal to the power radiated by the antenna when fed by the same current (Singh *et al.*, 2014).

Hence,

$$\boldsymbol{R_{rad} = \frac{2P_{rad}}{I^2}} \qquad \textbf{(}2.8\textbf{)}$$

$$\textbf{Or} \qquad \boldsymbol{R_{rad} = \frac{Wr}{I_{av}^2}}$$

where

$\mathbf{W_r}$ = Radiated power

$$\boldsymbol{I_{av}^{\ 2} = \frac{I_0}{2}} \qquad \textbf{(}2.9\textbf{)}$$

$\mathbf{I_0}$ is the peak-value of the feed-point current.

vii. Antenna Impedance (Input Impedance):

This is the impedance presented by an antenna at its terminals or the ratio of the voltage to current at a pair of terminals or the ratio of the appropriate components of the electric to magnetic fields at a point. Examine the input impedance at a pair of terminals which are the input terminals of the antenna. These terminals are designated as *a –b* shown in figure2.10.

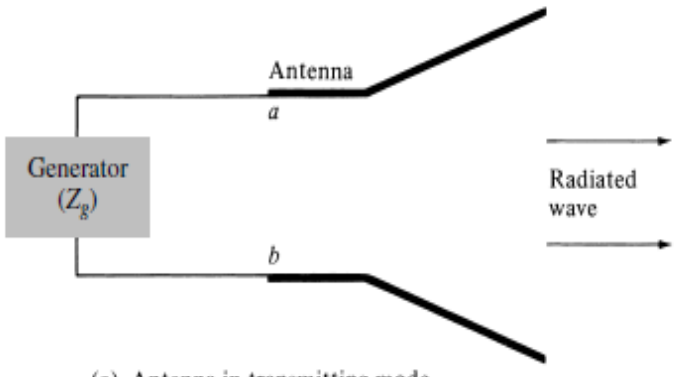

(a) Antenna in transmitting mode

`

Figure 2.10: Antenna in transmitting mode with its terminal impedance (Kraus, 1997)

According to Singh, Solanki, and Solanki (2014), the ratio of the voltage to current at these terminals, with no load attached, defines the impedance of the antenna as:

$$\boldsymbol{Z_A = R_A + jX_A} \quad (2.10)$$

Where,

$\boldsymbol{Z_A}$ = antenna impedance at terminals *a –b* (ohms)

$\boldsymbol{R_A}$ = antenna resistance at terminals *a –b* (ohms)

$\boldsymbol{X_A}$ = antenna reactance at terminals *a –b* (ohms)

The resistive part consists of two components; that is

$$\boldsymbol{R_A = R_r + R_L} \quad \textbf{(}2.11)$$

Where,

$\boldsymbol{R_r}$ = radiation resistance of the antenna

$\boldsymbol{R_L}$ = loss resistance of the antenna

For an efficient transfer of energy, the impedance of the transmitter or radio of the antenna and of the transmission cable connecting them must be the same. Transceivers and their transmission lines are typically designed for 50Ω impedance. If the antenna has an impedance different from 50Ω, then there is a mismatch and an impedance matching circuit is required.

viii. Directivity and Directive Gain:

`

Directivity is the ability of an antenna to focus energy in a particular direction when transmitting, or to receive energy better from a particular direction when receiving. In a static situation, it is possible to use the antenna directivity to concentrate the radiation beam in the wanted direction. However, in a dynamic system where the transceiver is not fixed, the antenna should radiate equally in all directions, and this is known as an omni-directional antenna. Directivity of an antenna is the maximum value of its directive gain. It is the ratio of the antenna's radiation intensity to the radiation intensity of an isotropic source as shown in equation (2.12). (Kraus, 1999; Singh *et al.*, 2014)

$$\boldsymbol{D_{max}} = \frac{\boldsymbol{U}}{\boldsymbol{U_O}} = \frac{\mathbf{4\pi\, U}_{\boldsymbol{max}}}{\boldsymbol{P_{rad}}} \qquad (2.12)$$

where,

U is the radiation intensity

U_O is the radiation intensity of an isotropic source

U_{max} is the maximum radiation intensity

P_{rad} is the radiated power

D_{max} is the maximum directivity

Gain is not a quantity which can be defined in terms of a physical quantity such as the Watt or the Ohm, but it is a dimensionless ratio. Gain is given in reference to a standard antenna. The two most common reference antennas are the isotropic antenna and the resonant half-wave.

Directive gain is defined as the ratio of antenna radiation intensity to that of a hypothetical isotropic radiator that radiates the same power equally in all directions. It is as shown in equation (2.13) . (Balanis, 2005)

`

$$\boldsymbol{D_{(\theta,\phi)} = \frac{4\pi\, U_{(\theta,\phi)}}{P_{rad}}} \quad ` \tag{2.13}$$

ix. Effective Area (Aperture):

This is used to describe the power capturing characteristics of the antenna when Electromagnetic wave strikes on it. The effective antenna area is the ratio of the available power at the terminals of the antenna to the power flux density of a plane wave incident upon the antenna, which is matched to the antenna in terms of polarization. If no direction is specified, the direction of maximum radiation is implied**.** Effective Aperture ($\boldsymbol{A_e}$) describes the effectiveness of an Antenna in receiving mode; it is the ratio of power delivered to receiver to incident power density. It is the area that captures energy from a passing Electromagnetic wave. An Antenna with large aperture ($\boldsymbol{A_e}$) has more gain than one with smaller aperture ($\boldsymbol{A_e}$) since it captures more energy from a passing radio wave and can radiate more in that direction while transmitting.

Consider an Antenna with an effective Aperture, $\boldsymbol{A_e}$ which radiates all of its power in a conical pattern of beam area $\boldsymbol{\Omega_A}$, assuming uniform field $\boldsymbol{E_a}$ over the aperture, power radiated. (Balanis, 2005)

$$\boldsymbol{P = \frac{{E_a}^2}{Z_0} A_e} \tag{2.14}$$

where Z_0 is the input impedance.

`

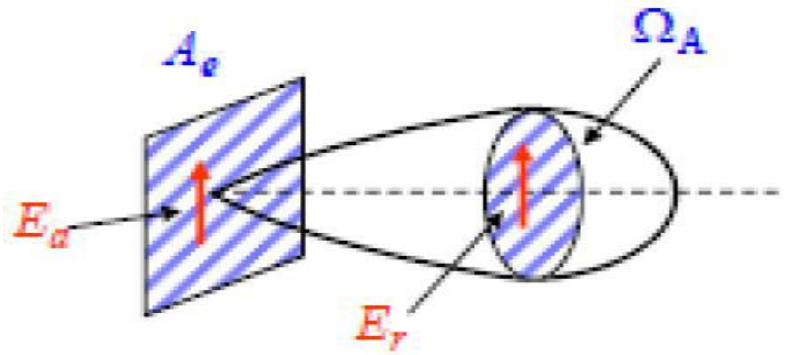

Figure 2.11: a diagram showing the effective area of an antenna (Balanis, 2005)

Assuming a uniform field $\mathbf{E_r}$ in far field at a distance **r**, Power Radiated is also given by (Balanis, 2005)

$$P = \frac{{E_r}^2}{Z_0} r^2 \Omega_A \qquad \textbf{(}2.15\textbf{)}$$

Equating the two and noting that $\mathbf{E_r = E_a A_e / r\lambda}$ the Aperture-Beam area relation is defined as, $\boldsymbol{\lambda^2 = A_e \Omega_A}$

At a given wavelength if Effective Aperture is known, Beam area can be determined and vice-versa.

Directivity in terms of beam area is given by $\boldsymbol{D = \frac{4\Pi}{\Omega_A}}$ (2.16)

Aperture and beam area is related by $\boldsymbol{\lambda^2 = A_e \Omega_A}$ **(**2.17)

Directivity can be written as $\boldsymbol{D = \frac{4\Pi A_e}{\lambda^2}}$ (2.18)

Hence the Effective Area is given as $\boldsymbol{A_e = \frac{\lambda^2 D}{4\Pi}}$ (2.19)

Where,

$\boldsymbol{A_e}$ = effective area (effective aperture) *(*m^2*)*

$\boldsymbol{\lambda}$ = Wavelength (m)

`

D = Directivity (dimensionless)

2.4 Magnetic Vector Potential

In the analysis of antenna radiation problems, the usual procedure is to specify the current sources, that is magnetic and electric current source (**J** and **M**) and then determine the fields radiated by the sources, whereas the reverse is the case for synthesis problems, where the radiated fields are specified and we are required to determine the sources. A very common practice in the analysis procedure is the introduction of Auxiliary functions known as *vector potential,* which aids in the solution of the problems. The most common vector potential functions are magnetic vector potential **A** and electric vector potential **F,** corresponding to the vector Hertz potentials Π_e and Π_h respectively. Once the vector potentials are known, then the electric and magnetic field intensities (E and H) can be determined because any well-behaved function, no matter how complex , can always be differentiated. Figure 2.12 shows the relationships between the current density sources (**J,M**), the auxiliary potential functions (**A**,**F**) and the radiated fields (**E,H**).

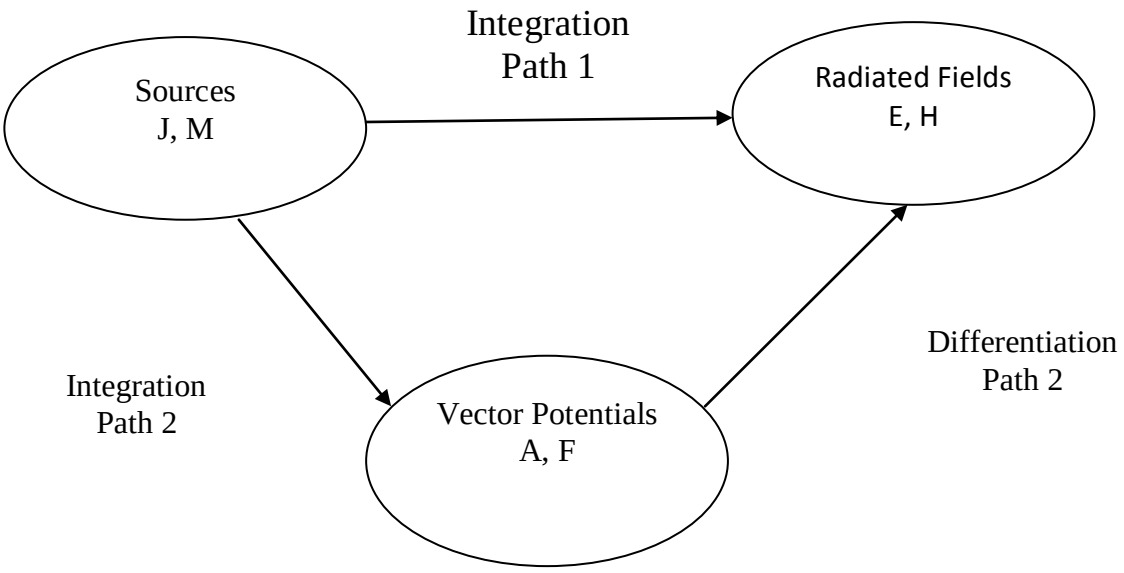

`

Figure 2.12: Computed Fields Radiated by Electric and Magnetic sources

The more frequently used magnetic vector potential, **A**, is defined such that the *curl* of **A** is the magnetic field **B**. Together with the *electric potential*, the magnetic vector potential can be used to specify the *electric field*, **E** as well. Therefore, many equations of electromagnetism can be written either in terms of the **E** and **B**, *or* in terms of the magnetic vector potential and electric potential. In more advanced theories such as *quantum mechanics*, most equations use the potentials and not the **E** and **B** fields. The vector **potential A** is useful in solving for the EM field generated by a given harmonic electric current source **J**. And, magnetic field is only a consequence of this potential (Balanis, 2005).

The magnetic vector potential **A** is a *vector field* defined along with the *electric potential* ϕ, (a scalar field) by the equations: (Balanis, 2005)

$$\boldsymbol{A} = \frac{\boldsymbol{\mu}}{\boldsymbol{4\pi}} \iiint \boldsymbol{J} \frac{\boldsymbol{e^{-jkR}}}{\boldsymbol{R}} \boldsymbol{dv'} \qquad \textbf{(}2.20\textbf{)}$$

Where,

A = Magnetic Vector Potential

J = Electric current density

$\frac{\boldsymbol{e^{-jkR}}}{\boldsymbol{R}}$ = Green's function

On the other hand, the Lorentz gauge equation is expressed as

`

$$\varphi = \frac{-\bar{\nabla}.\bar{A}}{j\omega\mu_0\varepsilon_0} \quad \textbf{(}2.21)$$

where,

μ_0 is the free space permeability

ε_0 is the free space permittivity.

2.5 Method of Moment (MoM)

Method of Moment is a numerical method which allows previously intractable complex antenna system configurations to be analyzed and designed very accurately. In addition, method of moment is one of the asymptotic methods for low frequencies. The Integral Equation Method casts the solution to the antenna problem in the form of an integral where the unknown, usually the induced current density, is part of the integrand. Numerical techniques, such as the Moment of Method (MOM), are then used to solve for the unknown (Balanis, 2005). Once the current density is found, the radiation integrals are used to find the fields radiated and other systems parameters. This method is most convenient for wire-type antennas and more efficient for structures that are small electrically. One of the first objectives of this method is to formulate the Integral Equation (IE) for the problem at hand. In general, there are two types of IE's. One is the *Electric Field Integral Equation (EFIE)*, and it is based on the boundary condition of the total tangential electric field. The other is the *Magnetic Field Integral Equation (MFIE)*, and it is based on the boundary condition that expresses the total electric current density induced on the surface in terms of the incident magnetic field. The MFIE is only valid on closed surfaces. For some problems, it is more convenient to formulate an EFIE, while

`

for others it is more appropriate to use an MFIE. Method of Moment (MOM) transforms integral equations to a set of simultaneous linear equations that are solved by matrix operation (Raida and Hudak, 1997). In antenna analysis and design, iterative method gives a rough approximation while Method of Moment offers very accurate result.

Summarized three steps involved in Method of Moment:

(a) Derivation of appropriate integral equations.

(b) Conversion or discretization of the integral equation into a matrix equation using basis or expansion functions and weighting or testing functions as well as evaluation of the matrix elements.

(c) Solving the matrix equation and obtaining the desired parameters (Kshetrimayum, 2016).

Method of Moment (MoM) finds application in: Antenna analysis and design, Population estimation in Statistics, Solving problem in Physics and Mathematics etc.

In February 2009 the FCC officially allowed the use of Method of Moment (MoM) modeling as a means of predicting self and driving point impedances of directional arrays, assuming they meet certain criteria (Federal Communications Commission, 2009**).** The moment method of modeling of antennas is an alternative to conventional field strength measurements as a means of performance verification. This alternative method has the potential of saving a tremendous amount of time and expense.

According to Alexander (2012), Moment method modeling has several benefits compared to the traditional ways of directional antenna analysis.

`

i. It solves for very close approximations of current distributions within a directional antenna. This is one of the most important advantage upon which all the other advantages emerge.

ii. Moment method technique forecasts antenna currents that are directly related to directional antenna parameters. Hence, it makes it possible to adjust the array to the desired parameters using antenna monitor parameters, provided that they accurately represent the antenna currents. This eliminates all the trial and error that is so much a part of the traditional array tune-up.

iii. Also, moment method predicts base driving point impedances very accurately which allows for close design of the phasing and coupling system. Moment method eliminates that guesswork, allowing the phasing and coupling system to be designed without all the "slack" for the unknowns. This is unlike in the use of traditional method in which the designing engineer will have to ensure large variations in current distribution and load impedance because the exact operating parameters required to produce the required antenna pattern is unknown.

2.6 Green's Function

Green's functions are named after the British mathematician George Green, who first developed the concept in the 1830s. In the modern study of linear partial differential equations, Green's functions are studied largely from the point of view of fundamental solutions instead. Under many-body theory, the term is also used in physics, specifically in quantum field theory, aerodynamics, aero

`

acoustics, electrodynamics, seismology and statistical field theory, to refer to various types of correlation function even those that do not fit the mathematical definition. In quantum field theory, Green's functions take the role of propagators.

In electromagnetism, the function gives an idea of how the current flowing through the antenna will appear in the far-field region. In this case the Green's Function Equation is written as:

$$\frac{e^{-jkR}}{R} \tag{2.22}$$

where

The far-field radiation patterns are determined by manipulating the $\hat{R}$ in the Green's function to $\hat{R} = |r - \hat{r}.\, r'|$

Where, r is the distance from the origin to the field point, and r' is the distance from the antenna source point to the field point. Thus,

Phase approximation is,

$$R = r - z_1' \cos\theta \tag{2.23}$$

Amplitude approximation is,

$$|R| \approx r \tag{2.24}$$

2.7 Review of Related Works

Weldon (2010) in his work entitled "A Direction Finding System Using Log Periodic Dipole Antennas in a Sparsely Sampled Linear Array", explored the use of Wide Band Log Periodic Dipole Array (LPDA) antennas in direction finding systems. The author deployed a novel approach utilizing non-uniform spacing in a linear array to improve the spatial resolution of the direction finding system. The linear arrays were referred to as minimum redundancy or non-redundant linear arrays. The author came up with results for the various sparse

`

array configurations which demonstrated good increase in the overall angular resolution of a phased array direction finding system. The author however assumed constant current sources in its analysis which were not practically obtainable. This antenna lacked precision.

In the work of (Segun *et al*., 2014) on Design and Numerical Analysis of a Single Half-Wave Dipole Antenna Transmitting at 235MHz Using Method of Moment, the authors dealt with the design and numerical analysis of a single Half- wave dipole antenna suitable for transmitting VHF television signals at a frequency of 235MHz using Method of Moment. The authors employed the radiating field and the electric field strength equations to determine the variations in the electric field strength and free space loss with distance in kilometers. Parameters such as the power radiated, gain and voltage standing wave ratio of the antenna were also evaluated. The radiation patterns obtained indicated that the antenna radiated well. The variations of electric field strength and free space loss with distance indicated the rate of loss of the signal transmitted at this particular frequency using half –wave dipole antenna. It is noted that the design was not basically for direction finding antenna system though Method of Moment approach was used.

Ozec (2011) on "Direction Finding Performance of Antenna Arrays on Complex Platforms Using Numerical Electromagnetic Simulation Tools", presented a method for both modeling and simulation in a numeric electromagnetic simulation tool FEKO (This is derived from the German acronym: **FE**ldberechnung für **K**örper mit beliebiger **O**berfläche). The method depended

`

on the data generated by FEKO. The data was processed by correlative interferometer algorithm; and implemented in a MATLAB environment. The author used different types of antenna arrays and evaluated the direction finding performance for different scenarios. This approach was effective for understanding the direction finding characteristic of antenna arrays but undermine the importance of antenna current accuracy on the system's performance.

Guerin et al. (2012) on "Passive Direction Finding: A Phase Interferometry Direction Finding System for an Airborne Platform", the authors described the development of a phase interferometry direction finding system for an airborne platform developed for MIT Lincoln Laboratory. A phase interferometer uses the phase difference to determine the Angle of Arrival (AoA) of a received signal, but is unable to distinguish phase differences of more than one period, giving rise to phase ambiguities. The team used three antennas to resolve phase ambiguities and was able to determine the azimuthal AoA for a received electromagnetic signal in the X band to within $\pm 0.1^0$ in simulations including realistic noise models for a 170^0 field of view. A prototype was implemented using a Field-Programmable Gate Array (FPGA) based board for data acquisition connected via Universal Serial Bus (USB) to a Personal Computer (PC) for analysis, which connected to another PC via a TCP connection for tracking and display. The hardware was only able to utilize two channels. Also, the authors focused on improving the circuitry of the direction finding system rather than on its antenna. These limitations resulted in ambiguous solutions in AoA calculations.

`

In the work of Mohammad and Daniel (2011), the authors presented the design and fabrication of an 8-element circular printed yagi antenna array that was operated in switched mode for a radio frequency direction finding system in vehicular platforms. The antenna array was designed to operate in the 2.45 GHz frequency band. The directional gain patterns have a Half Power Beam Width (HPBW) between 65 - 110 degrees in the azimuth plane which was used to identify the direction of the incoming Radio Frequency (RF) signal from one of 8 sectors using the power based method algorithms. Two simulation models were created to study the effect of a Ground (GND) split introduction in the array GND plane between every two adjacent elements. The introduction of the splits enhanced the directivity of the array, increased the operating BW, enhanced the maximum gain, and lowered the back lobe radiation by at least 5 dB.

Jun-Ho, Joon-Ho, Cheol-Sun, and Seung-Sub (2006) on "Active Composite Dipole Antenna for Direction Finding Array Antenna Applications" emphasized that an accurate direction finding (DF) detection was required for measuring and analyzing the physical parameters of the Radio Frequency (RF) signals in the dense signal environment. According to the authors, the main element of the DF system was the antenna unit, which should be carefully designed because the sensitivity of the DF system was dependent on the gain and the radiation patterns of the antenna and the characteristics of the antenna arrays. The authors presented the broadband active composite dipole antenna for applications requiring a low profile, lightweight and compact direction finding array. The

`

antenna played a role in two dipoles functionally and also one dipole physically to improve the gain in the V/UHF-band. This type of antenna had a high gain more than that of one dipole antenna within limited length. It was useful for the direction finding system because of compact and broadband.

2.8 Research Gaps

i. The importance of accuracy on antenna current was undermined on the system's performance analysis. It could lead to detection of false alarms by the DF system.

ii. Half wave dipole antenna could not perform well in direction finding system due to its narrow band and low directivity. The phased arrays are preferred because sharper nulls can be obtained with phased arrays. Phased arrays are somewhat less sensitive to propagation effects, possibly because of their larger size for the same frequency of operation and thus offer some space diversity.

iii. Constant current sources are not practically obtainable in antenna operation. All the antenna system parameters are dependent on the source current flowing through the elements of the antenna. For better analysis of antenna behaviour, exact or near current value is required, and not an assumed constant current source.

The use of Method of Moment guarantees the generation of an approximate current distribution for a direction finding system antenna which helps to minimize the detection of false alarms by the DF system.

`

Also, the use of Yagi-Uda antenna would correct the problem of narrow band and low directivity because of its wide band and also ensure an improved directivity.

CHAPTER THREE

METHODOLOGY

This chapter discusses the method of moment technique along with the Magnetic Vector Potential operator used in the analysis of the current flowing through the array antenna elements. It also enumerates the procedures followed in the design of the yagi array antenna. In the design considerations, it is ensured that the power supplied by the transmitter is not wasted. Thus, the antenna elements possess exact dimensions which are determined by the transmitting frequencies, and as such ensure proper antenna pattern orientation. The design considerations are detailed in the design section of 3.2.

The Moment Method technique helps to derive the approximate current flowing through the antenna elements while the Magnetic Vector Potential operator is employed as it contains an auxiliary function that eases the analytical procedures.

3.1 Generation of the Current Distribution Using Method of Moment and Magnetic Vector Potential Operator

The Method of Moment (MoM) approach is employed in connection with the Magnetic Vector Potential (MVP) operator in analyzing the current flowing through the antenna elements. The role of the Method of Moment on the Yagi antenna is to obtain the mathematical equations describing the Yagi antenna

`

array and then to convert the equation into matrix equations suitable for computer simulation.

In method of moment modeling of an antenna, the antenna element was divided up into segments. The antenna segment currents were then solved numerically, taking cognizance of the field coupling between segments on the radiator and the currents conducted from adjacent segments.

3.1.1 Method of Moment (MoM)

Numerical solutions of electromagnetic field problems are generally classified into two groups namely:

i. The direct solutions for the electromagnetic fields, and
ii. The solution for the field sources.

In both cases, the equations that are to be solved are linear operator equations in terms of the unknowns (the fields, viz. the sources). (Sarkar, Djordjevic and Kolundzija, 2000)

While the equations are differential in the first scenario, the second case is integral. However, both classes of equations belong to the general class of linear operator equations, which have the common form

$$L(f) = g, \tag{3.1}$$

where L is the operator, g is the source or excitation, which is assumed to be a known function, and f is the field or response, which is the unknown function to be determined. The linearity of the operator emanates from the linearity of Maxwell's equations and the constitutive equations.

Thus, for the first group of numerical methods L is a differential operator. It generally involves derivatives with respect to three spatial coordinates. Also, f

`

is a field vector or potential, and g is a known quantity such as the field or potential due to an incident wave (Sarkar *et al*., 2000).

For the second group of numerical methods L is an integral operator, f represents the field sources, and g is, again, a known quantity that models the excitation.

Hence, the operator equation (3.1) can be solved following the numerical method known under the generic name of the method of moments (MoM), which is a general technique for solving linear operator equations.

3.1.1.1 Basic steps of the method of moments

The unknown quantity (f) is expanded in terms of a set of linearly independent known functions, fn. That is, it is approximated by the following finite series:

$$f = \sum_{n=1}^{N} \alpha_n f_n \tag{3.2}$$

where $\alpha_n$are unknown coefficients to be determined. The expansion functions should be selected, such that reasonable approximation of f is obtained with a small number of terms, N.

i. Substitute equation (3.2) into (3.1), to obtain the approximate equation

$$L(\sum_{n=1}^{N} \alpha_n f_n) \approx g \tag{3.3}$$

Owing to the linearity of the operator, equation (3.3) can be rewritten as

$$\sum_{n=1}^{N} \alpha_n L f_n \approx g \tag{3.4}$$

The unknown coefficients, αn, should now be determined such that equation (3.4) is satisfied.

ii. A measure is needed describing the degree of accuracy to which the left side and the right side of equation (3.4) match. Thus, both sides of equation (3.4) are multiplied by a known, properly selected function,

`

referred to as the weighting function, *wm* , and the results integrated over a spatial region. This produces equation (3.5)

$$\sum_{n=1}^{N} \alpha_n < w_m, L(f_n) >=< w_m, g > \quad (3.5)$$

The inner products in equation (3.5) are definite numbers which can be evaluated analytically or numerically. Hence, equation (3.5) represents a linear equation in coefficients α*n.*

To obtain a determined system of linear equations for these coefficients, the weighting procedure is done for a linearly independent set of *N* functions, yielding

$$\sum_{n=1}^{N} \alpha_n < w_m, L(f_n) >=< w_m, g >, \text{ m=1……N.} \quad (3.6)$$

Equation (3.6) represents a system of *N* ordinary linear equations in *N* unknowns, and it can be solved using various techniques.

The techniques based on integral equations result in compact, but full systems, which are usually solved using the Gaussian elimination or similar techniques, like the LU decomposition.

3.1.2 Magnetic Vector Potential

The Magnetic Vector Potential (MVP) model of equation **(**2.20) was used in the analysis of the antenna current as it contains Green's function, which is a linear operator. The MVP model makes use of auxiliary functions which helped in the solution for the antenna current. Also, the Magnetic Vector Potential (MVP) approach was used in the analysis of the antenna parameters.

The yagi antenna segment length in Figure 3.1 was carefully selected and a close approximate value of the actual current distribution was obtained from the

`

model. Thus, this has the benefit of forecasting base drive impedances much more correctly than any other method.

A conventional diagram for the analysis of the yagi antenna current and parameters is shown in Figure 3.1. The elements of the Yagi array are positioned along the Z-axis on the Cartesian plane.

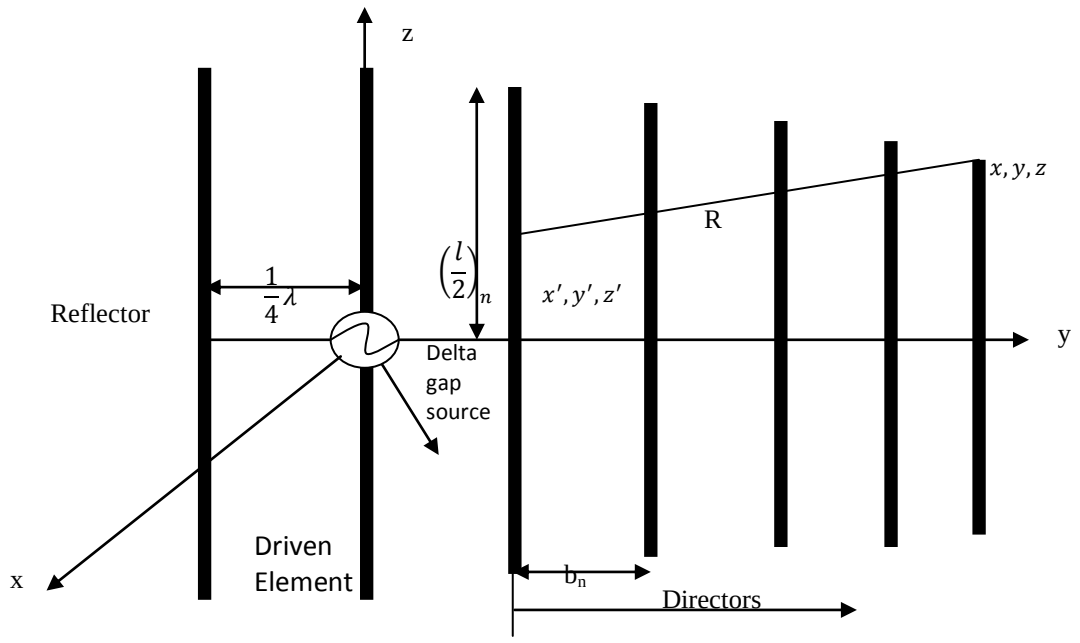

Figure 3.1: Diagram of the Yagi array along the Z-axis on the Cartesian plane

Hence, the conventional Magnetic Vector Potential equation is generally expressed as (Balanis, 2005)

$$\bar{A} = \iiint \bar{J}(r') \left[\exp(-jk_0 R) / R \right] dv' \tag{3.7}$$

`

And from equation **(**2.21), the Lorentz gauge equation is expressed as in (Raida and Hudak, 1997)

$$\varphi = \frac{-\bar{\nabla}.\bar{A}}{j\omega\mu_0\varepsilon_0} \tag{3.8}$$

where,

ε_0 represents free space permittivity,

μ_0 is the free space permeability,

k_0 represents the free-space propagation constant,

R is the distance from source to field point,

$\bar{J}$ is the electric current density,

dv' is the elemental volume of the radiating wire,

$\frac{e^{-jk_0R}}{R}$ is the free space Green's function,

j is the imaginary number and

ω is the angular frequency in radians per second.

r' is the distance between the antenna origin to the far field point.

Note: Lorentz guage condition offers the relationship between the current and charge distributions by the equation of continuity.

If the antenna is electrically thin, that is, its radius (a) is much smaller than wire length (l) and wavelength (λ), the usual thin-wire approximations can be used with the wire antenna lying along the z axis. Thus, for a symmetric, center-fed linear dipole antenna, the vector potential has only a z component (McDonald, 2009). Then, equation (3.7) then becomes

$$A_z = \frac{\mu_0}{4\pi}\int_{-\frac{l}{2}}^{+\frac{l}{2}} I(Z')\frac{e^{-jk_0R}}{R}\,dz' \tag{3.9}$$

`

$I(z')$ is the filamentary source current on the radiating wire

From Lorentz guage condition of equation (3.8),

$$\varphi = \frac{-1}{j\omega\mu_0\varepsilon_0}.\frac{\partial A_z}{\partial z} \tag{3.10}$$

Stage 1:

The scattered electric field intensity symbolized by E^s, as a result of an induced current due to an impressed field on the surface of a perfectly conducting wire that is transmitting in free space is represented in equation (3.11). (McDonald, 2009)

$$E^s = -j\omega\bar{A} - \bar{\nabla}\varphi \tag{3.11}$$

where

$\bar{A}$ is the magnetic vector potential,

φ is the electric scalar potential and

$\bar{\nabla}$ is del or gradient operator.

Thus,

$$E^s(z) = -j\omega A_z - \frac{\partial\varphi}{\partial z} \tag{3.12}$$

Substituting equation (3.10) in equation (3.12), we have

$$E^s(z) = -j\omega A_z + \frac{1}{j\omega\mu_0\varepsilon_0}.\frac{\partial^2 A_z}{\partial z^2} \tag{3.13}$$

Substituting the linear operator of equation (3.9) into the unknown quantity of equation (3.13), will result to equation (3.14)

$$E^s(z) = jw\mu_0 \int_{-\frac{l}{2}}^{+\frac{l}{2}} I(Z')\frac{e^{-jk_0R}}{4\pi R}\,dz' + \frac{1}{jw\varepsilon_0}\frac{\partial^2}{\partial z^2}\int_{-\frac{l}{2}}^{+\frac{l}{2}} I(Z')\frac{e^{-jk_0R}}{4\pi R}\,dz' \tag{3.14}$$

`

Note: For wire antennas, order of integration and derivation can be swapped (Sarkar, Djordjevic and Kolundzija, 2000).

Remember the antenna relation: ($k = w\sqrt{\mu_0 \varepsilon_0}$), thus, for convenience, equation (3.14) can be rewritten as shown in equation (3.15),

$$E^s(z) = \frac{1}{jw\varepsilon_0}\left\{\frac{\partial^2}{\partial z^2}\int_{-\frac{l}{2}}^{+\frac{l}{2}} I(Z')\frac{e^{-jk_0R}}{4\pi R}\,dz' + k_0^2\int_{-\frac{l}{2}}^{+\frac{l}{2}} I(Z')\frac{e^{-jk_0R}}{4\pi R}\,dz'\right\} \quad (3.15)$$

where k is the free space wave number

From one of the conventional antenna equations,

$$\frac{1}{\omega\varepsilon_0} = \frac{\eta_0}{k_0} \quad (3.16)$$

(Balanis, 2005)

Hence, substituting equation (3.16) into (3.15) results to

$$E^s(z) = \frac{\eta_0}{jk_0}\left\{\frac{\partial^2}{\partial z^2}\int_{-\frac{l}{2}}^{+\frac{l}{2}} I(Z')\frac{e^{-jk_0R}}{4\pi R}\,dz' + k_0^2\int_{-\frac{l}{2}}^{+\frac{l}{2}} I(Z')\frac{e^{-jk_0R}}{4\pi R}\,dz'\right\} \quad (3.17)$$

where,

η_0 is the intrinsic impedance of free space

Therefore, equation (3.17) can be rearranged as shown in equation (3.18)

$$E^s(z) = \frac{\eta_0}{jk_0}\left\{I(Z')\int_{-\frac{l}{2}}^{+\frac{l}{2}}\left[\frac{\partial^2}{\partial z^2}\left(\frac{e^{-jk_0R}}{4\pi R}\right) + k_0^2\left(\frac{e^{-jk_0R}}{4\pi R}\right)\right]dz'\right\} \quad (3.18)$$

For convenience, it can further be expressed as in (Adekola, and Raji, 2017).

Thus,

$$E^s(z) = \frac{\eta_0}{jk_0}\int_{-\frac{l}{2}}^{+\frac{l}{2}} I(Z')\left\{[(1+jk_0R)(2R^2-3a^2) + k_0^2R^2a^2]\frac{e^{-jk_0R}}{4\pi R^5}dz'\right\} \quad (3.19)$$

where,

R is the distance of the antenna from the observation point to the far field zone.

`

a is the diameter of the antenna element.

For a perfectly conducting element, the tangential electric field become extinct on the surface of the wire, and the boundary condition suitable to the average tangential electric field is represented in equation (3.20) as (Balanis, 2005)

$$n \times E^t(z) = n \times \left(\left[E^s(z) + E^i(z)\right] = 0\right) \quad (3.20)$$

where,

n is the unit vector normal to surface

E^t is the tangential electric field.

For the scattered electric field intensity to fulfill the boundary conditions on the antenna surface S,

This will eventually result to equation (3.21) as the tangential component of the electric field becomes zero or vanishes.

$$E^i(z) = -E^s(z) \quad (3.21)$$

where

$E^i(z)$ is the incident electric field.

Substituting equation (3.19) into equation (3.21), we have

$$E^i(z) = \frac{\eta_0}{jk_0} \int_{-\frac{l}{2}}^{+\frac{l}{2}} I(Z') \left\{ [(1 + jk_0R)(2R^2 - 3a^2) + k_0^2R^2a^2] \frac{e^{-jk_0R}}{4\pi R^5} dz' \right\} \quad (3.22)$$

The electric field integral equation for a wire antenna is represented in equation (3.22) whose only unkown is $I(z')$.

(That's: $E^i(z) = L[I(Z')]$; where L is the linear operator

Stage 2:

`

It should be noted that the Yagi antenna array has a single driven element on which the excitation source is located as shown in figure 3.1. The electric field supplied by the excitation source induces current on all the elements of the array because there is mutual coupling between the elements of the array. Also, all the elements of the yagi antenna are perfectly conducting and energized by the supply on the driven element.

Thus, applying the summation operation, the integral equation for the N-element array represented in figure 3.1 is as shown in equation (3.23)

$$E^i(z) =$$

$$\frac{\eta_0}{jk_0}\sum_{n=1}^{N}\int_{-\frac{l_n}{2}}^{+\frac{l_n}{2}} I_n(z_n^{'})\left\{[(1+jk_0R)(2R^2-3a^2)+k_0^2R^2a^2]\frac{e^{-jk_0R}}{4\pi R^5}dz_n^{'}\right\} \tag{3.23}$$

In view of the fact that there are N elements in the antenna array, there will be N equations for n=1, 2, 3, …….. N

Since the current distribution of a symmetrical dipole is an even function, the distribution can be approximated by cosine terms of Fourier series.

Also, when the unknown current $I_n(z_n')$ is approximated by current coefficient, the entire domain basis function as used elsewhere becomes (Raida and Hudak, 1997)

$$I_{nm}(z_n^{'}) = \sum_{m=1}^{M} I_{nm}cos\left[\frac{(2m-1)\pi z_n^{'}}{2\left(\frac{l}{2}\right)_n}\right], \text{m} = 1,2,3 \ldots . \text{M} \tag{3.24}$$

where

I_{nm} stands for the complex current coefficient of mode m on element n

where

m=1,2,…, N-1.

`

The Dirac function was employed as weighting function. Its inner product was taken with equation (3.23) as shown in Appendix A to generate equation (3.25).

$$\int_{-\frac{l}{2}}^{+\frac{l}{2}} w_p E^i(z)dz = \frac{j\eta_0}{k_0} \sum_{n=1}^{N} \sum_{m=1}^{M} I_{nm} \int_{-\frac{l_n}{2}}^{+\frac{l_n}{2}} cos\left[\frac{(2m-1)\pi z_n^{'}}{2\frac{l_n}{2}}\right] \left[(1 + jk_0R_{np})(2R_{np}^2 - 3a^2) + k_0^2R_{np}^2\, a^2\right] \frac{e^{-jk_0R_n}}{4\pi R_{np}^5} dz_n^{'} \quad (3.25)$$

where

$$R_{np} = \sqrt{\rho^2 + (z - z')^2} \quad (3.26)$$

and,

R_{np} is the distance from the elemental antenna to the far field point.

ρ is the distance from the centre feed of the elemental antenna to the ground of the far field point.

z is the distance from ground at the far zone to the far field point

$z^{'}$ is the distance from the elemental antenna source to the far field point.

Note: This approach allows for direct investigation of the current distribution, but not the input impedance. Computing the matrix equation (3.25) produces the Fourier coefficients of the current distribution program in the matlab syntax.

Alternatively,

Equation (3.23) is known as Electric Field Integral Equation (EFIE) which can be written in the form represented by

$$E^i(z) = L[I(z)'] \quad (3.27)$$

where,

`

$$L[I(z)'] =$$

$$\frac{\eta_0}{jk_0}\sum_{n=1}^{N}\int_{-\frac{l_n}{2}}^{+\frac{l_n}{2}} I_n(z_n^{'})\left\{[(1+jk_0R)(2R^2-3a^2)+k_0^2R^2a^2]\frac{e^{-jk_0R}}{4\pi R^5}dz_n^{'}\right\} \quad (3.28)$$

To determine the current distribution on Yagi-Uda antenna, the unknown current $I(z)^{'}$ in eqn. (3.28) is expanded in terms of unknown complex coefficient I_{ns} and known expansion function J_{ns} of the form represented by

$$I(z)^{'} = \sum_n \sum_s I_{ns} J_{ns} \quad (3.29)$$

provided , n=1, 2, 3, …N and s=1, 2, 3, 4, ….S.

where,

n is the number of elements in the array and

s is the number of expansion functions.

Substituting eqn. (3.29) into eqn. (3.27) and invoking the linearity property of operator L yields an expression of the form

$$E^i(z) = \sum_n \sum_s I_{ns} L[J_{ns}] \quad (3.30)$$

Equation (3.30) is not sufficient to determine the current distribution of interest; therefore, an inner product of eqn. (3.20) is taken with dirac delta weighting function ($f_{nk} = \partial(z_n^{'} z_m)$).

Hence,

$$< f_{nk}\, E^i(z) > = \sum_n \sum_s I_{ns} < f_{nk} L[J_{ns}] > \quad (3.31)$$

where,

m is the discrete points within which the boundary condition is enforced.

Equation (3.28) can be written in compact form as represented in equation (3.32)

$$V_{nk} = I_{ns} Z_{(nk),(ns)} \quad (3.32)$$

where,

`

V_{nk} is the voltage matrix (This represents entries that account for antenna's excitation as a result of the impressed field),

The feed on the driven element was modeled by Delta-gap model with a feed voltage of 1Volt. Also, the entries into voltage matrix are zeros except at the feedpoint.

$Z_{(nk),(ns)}$ is the impedance matrix (It is made of elements formed by the inner product of testing function with integral on basis function).

I_{ns} is the unknown current coefficient

Thus, from equation (3.32), equation (3.33) is obtained as shown;

$$\begin{bmatrix} V_1 \\ V_2 \\ V_3 \\ \vdots \\ V_k \end{bmatrix} = \begin{bmatrix} I_1 \\ I_2 \\ I_3 \\ \vdots \\ I_k \end{bmatrix} \begin{bmatrix} Z_{11} & Z_{12} & Z_{13} & \dots & Z_{1k} \\ Z_{21} & Z_{22} & Z_{23} & \dots & Z_{2k} \\ Z_{31} & Z_{32} & Z_{33} & \dots & Z_{3k} \\ \vdots & \vdots & \vdots & \dots & \vdots \\ Z_{k1} & Z_{k2} & Z_{k3} & \dots & Z_{kk} \end{bmatrix} \quad (3.33)$$

The system of matrix equations was then solved to find the complex coefficient of the current distribution on each wire by finding the product of the voltage matrix and the inverse of an impedance matrix.

For the Yagi antenna array consisting of a reflector, a dipole, and *k*-3 directors, all the voltages in the vector except V_2 become zero. V_2 is set to 1 unit; the voltage vector can be written as $[V] = [0,1,0,...0]^T$, so that the currents in the elements *I*1, *I*2 ,...,*Ik* can be calculated as represented in equation (3.34).

$$[I_{ns}] = \left[Z_{(nk),(ns)}\right]^{-1}[V_{nk}] \quad (3.34)$$

Equation (3.34) is usually solved using the Gaussian elimination or similar techniques, like the LU decomposition.

`

Hence, software implementation of equation (3.25) or equation (3.34) produces the unknown currents. The current values obtained are substituted in the designed antenna equations for analyzing the antenna parameters.

Note: The classical matrix inversion is an inefficient technique, as it requires about three times more operations, and hence three times longer CPU time, than the Gaussian elimination. Large full MoM systems of linear equations have also been successfully computed using other techniques, such as the conjugate gradients alone or in combination with the fast Fourier transform (Sarkar *et al.,* 2000). The flowcharts for the MoM Technique and for the antenna current generation are as shown in figures 3.3 and 3.4 respectively.

`

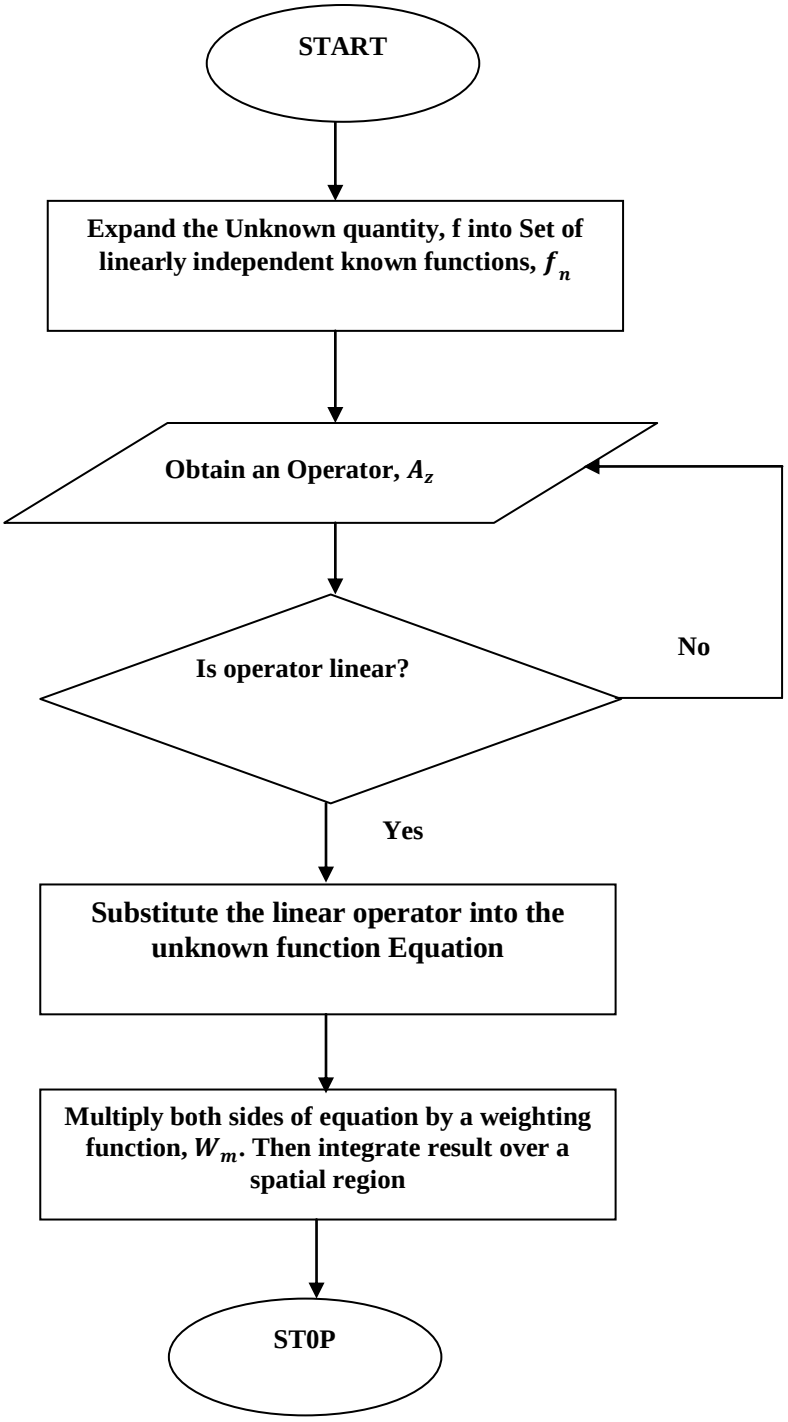

Figure 3.3: Flowchart for the MoM Technique

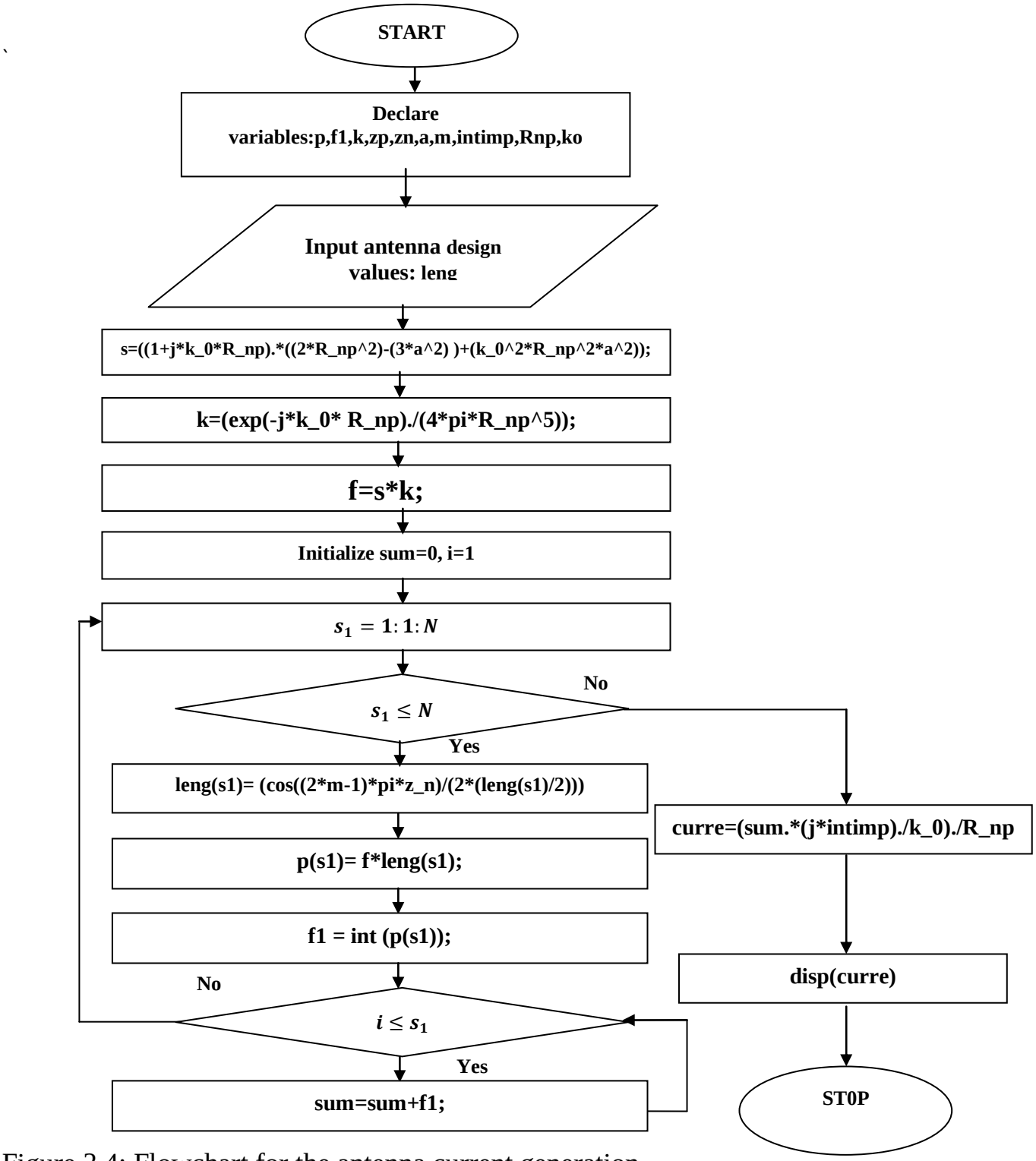

Figure 3.4: Flowchart for the antenna current generation

`

3.2 Design of a Direction Finding System Yagi Antenna

In designing the antenna for DF systems, care is taken to ensure that the antenna is able to radiate efficiently. This also ensures that the power supplied by the transmitter is not wasted. For an antenna to radiate efficiently, the antenna elements possess exact dimensions which are determined by the transmitting frequencies. When an antenna is in the receiving mode, its dimensions do not really matter for relatively low radio frequencies. The situation is different when the frequency of the signal to be received increases. In this case, the design and installation of such antenna become challenging.

This section in Chapter three highlights the design of the proposed Yagi antenna for a Direction Finding system. In antenna design, it is usually conventional to first consider the frequency in which the antenna is to be operated. Thus, the DF antenna under consideration is meant for Ultra High Frequency (UHF) applications which must lie within the frequency range of 0.3 GHz to 3GHz. For experimental purpose, this research considered the frequency band of 0.6GHz to 0.8GHz in the design of the yagi antenna. Also, varying dipole antenna lengths and spacing between the reflector, dipoles and directors where considered.

3.2.1 Design Procedures for the Yagi Antenna

There are a number of approaches that is considered in order to extend the bandwidth of the yagi array. Such measures taken include:

i. Selection of the driven dipole for midband operations
ii. Increasing the length of reflector for low frequency operations
iii. Reduction of the length of directors for high frequency operations

`

It should be observed that the parasitic elements (directors) were used basically to enhance gain at the upper and lower frequency limits of the reflecting element.

3.2.1.1 Resonant Length of the Antenna

The desired resonant length of the antenna was obtained at the frequency of operation because an antenna behaves as a resonant circuit. The resonance occurs as electrons travel from the centre of a centre fed antenna of length l meters to the end and back in a time equivalent to that occupied by one half of input cycle.

Thus,

$$t = \frac{l}{c} \text{ secs} \tag{3.35}$$

Also,

$$t = \frac{1}{2f} \text{ secs} \tag{3.36}$$

When the antenna is operating at resonance, the time of operations above are equivalent. Hence

$$\frac{l}{c} = \frac{1}{2f} \tag{3.37}$$

Rearranging the equation,

$$l = \frac{c}{2f} \tag{3.38}$$

and

$$f = \frac{c}{2l} = \frac{c}{\lambda} \tag{3.39}$$

where,

c is the speed of light in meters/second

λ is the wavelength in meters

`

f is the frequency in Hertz.

The physical interpretation of this is that, an antenna of length, $\frac{\lambda}{2}$ meters will perform as a resonance circuit thereby generating large amplitude voltages and currents. This will result to the radiation of strong electromagnetic wave.

3.2.1.2 Center frequency

For $f_1 = 0.6GHz$ and

$f_2 = 0.8GHz$

The center frequency for the antenna is computed thus,

$$f_c = \sqrt{f_1 \times f_2} \tag{3.40}$$

(Taylor and Huang, 1997).

The above formular was employed because the ratio of f_2 to f_1 is greater than 1.11. That is, $\frac{f_2}{f_1} > 1.11$, otherwise the formular should be , $f_c = \frac{f_1 + f_2}{2}$.

Hence,

$f_c = \sqrt{0.6GHz \times 0.8GHz} = 0.693GHz$

The center frequency is $0.693GHz$

3.2.1.3 Length (L) of the dipole

The length (L) of the dipole was computed using the center frequency of 0.693GHz

For resonance to be attained, the length of the dipole required depends on the frequency as well as, to a lesser extent, on the ratio of the diameter of the element to the wavelength. Hence, from the relation

$$\lambda = \frac{c}{f} \tag{3.41}$$

where, c= frequency of light (m)

`

f=center frequency (Hz)

$$\lambda = \frac{3\text{X}10^8\ (m)}{693{,}000\ (MHz)} = 0.43\ m$$

$$l = \frac{\lambda}{2} = \frac{0.43}{2} = 0.22\ m$$

3.2.1.4 Length (L) of the Reflector

The length of the reflector was calculated from the lower frequency of the band to be detected by the direction finding system, that is 0.6GHz. Thus, the wavelength of the reflector was calculated as shown below,

$$\lambda = \frac{3\text{X}10^8\ (m)}{600{,}000{,}000\ (Hz)} = 0.5\ m$$

Also, the length of the reflector was as below

$$l = \frac{\lambda}{2} = \frac{0.5}{2} = 0.25\ m$$

3.2.1.5 Length of the smallest director

The length of the smallest director was calculated by the use of the highest frequency 0.8GHz

$$\lambda = \frac{3\text{X}10^8\ (m)}{800{,}000{,}000\ (Hz)} = 0.375\ m$$

$$l = \frac{\lambda}{2} = \frac{0.375}{2} = 0.188\ m$$

In order to ensure optimum performance, the lengths of the directors should vary between the lengths of dipole of 0.22m to the smallest length (due to the highest director length of 0.19m). The lengths of the elements in the high-

`

frequency array are shorter than those in the low-frequency array as shown in Tables 3.1, 3.2 and 3.3.

(This variation can be viewed from this wave equation, $f = \frac{c}{\lambda} = \frac{c}{2l}$).

where c and λ are constants.

Thus, $f \infty \frac{1}{l}$

For experimental and testing purpose, reduction of 2%, 3% and 4% were chosen as multipliers for the length of the directors from the dipole (Patidar, Singhal, Gupta, and Prjapati, 2012).

The above choice was made to enable gradual decrease in length of the directors which ensured that the beam is radiated in the desired direction. It also allowed for minimal number of directors required for the antenna design within the frequency of operation.

Therefore, for the dipole length of 0.22m,

2% reduction resulted to

=0.02×0.22m =0.0044m

The 2% variation resulted to seven directors of length as shown in Table 3.1

Table 3.1: Lengths of director with 2% reduction

Directors	D1	D2	D3	D4	D5	D6	D7
Lengths(m)	0.216	0.211	0.207	0.202	0.198	0.194	0.189

For 3% reduction, we have

=0.03×0.22m =0.007m

This also generated four directors of lengths given in Table 3.2.

`

Table 3.2: Lengths of director with 3% reduction

Directors	D1	D2	D3	D4
Lengths(m	0.213	0.206	0.199	0.192

Also, for 4% reduction, we have

=0.04×0.22m =<u>0.009m</u>

This also resulted to three directors of lengths given in Table 3.3.

Table 3.3: Lengths of director with 4% reduction

Directors	D1	D2	D3
Lengths(m)	0.211	0.202	0.193

3.2.1.6 Reflector to Dipole Spacing/ Dipole to director Spacing

A spacing of 0.25wavelength was used in-between the antenna Dipole and its reflector.

Hence,

0.25×0.43 m (wavelength of the center frequency) =<u>0.108m</u>

The choice of the above spacing was made in order to achieve most reflection that will ensure high gain.

Also, in designing for the spacing from the antenna dipole to the first director, and then between the directors, a spacing of 0.2 wavelength was

`

employed in order to allow use of more directors (Patidar, Singhal, Gupta, and Prjapati, 2012).

Thus, 0.2×0.43 m =0.086m

Hence, applying 4% reduction in spacing the remaining directors, we have;

0.04x0.086=0.0172m

The result of the spacing was tabulated in Table 3.4

Table 3.4: Spacing between the reflector, dipole and directors (D1, D2, and D3)

Directors	Reflector – Dipole	Dipole – D1	D1 – D2	D2 – D3
Spacing (m)	0.108	0.086	0.069	0.052

In the design, the choice of lengths of director with 4% reduction was made because of its compactness as a result of lesser number of parasitic elements. This left us with having only five elements comprising a reflector, a dipole and three (3) directors.

In conclusion to this, the lengths of the reflector, dipole, and the three (3) directors along side with the spacing were tabulated in Table 3.5. These values were used and simulated using The Matlab software tools. The results of the simulation were presented and analyzed in Chapter four.

`

Table 3.5: Length and Spacing between the reflector, dipole and directors

	Reflector	**Dipole**	**Directors**		
			D1	D2	D3
Lengths (m)	0.25	0.22	0.211	0.202	0.193
		Reflector – Dipole	Dipole – D1	D1 – D2	D2 – D3
Spacing (m)		0.108	0.086	0.069	0.052

The diagram of the designed five element Yagi array antenna for the study is shown in Figure 3.2.

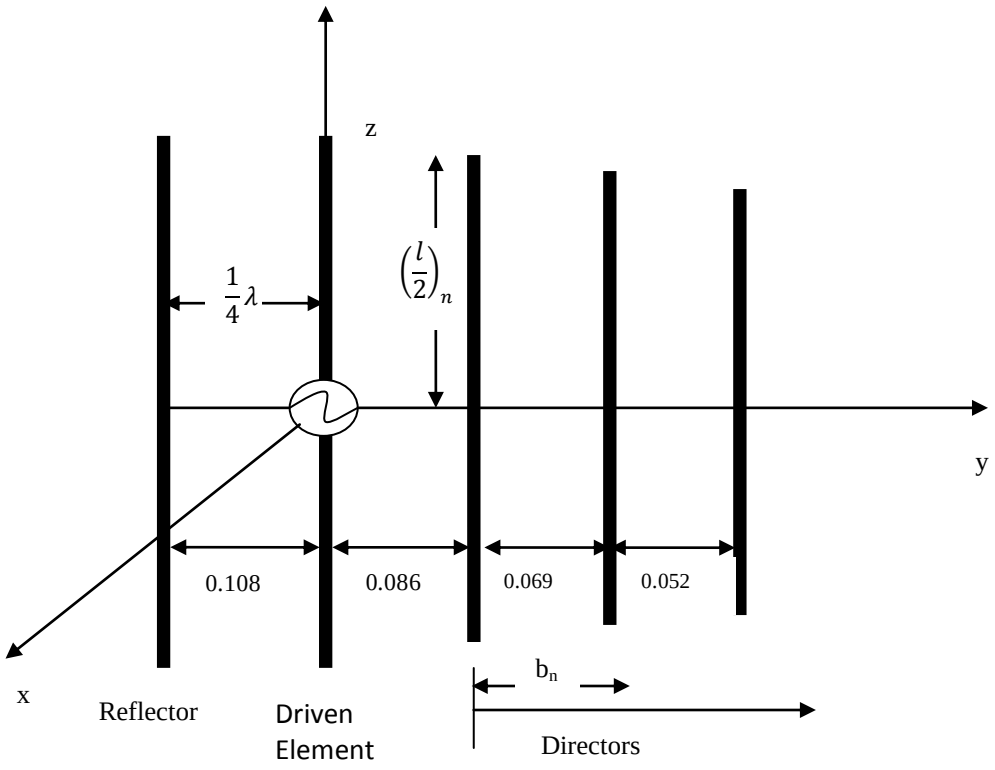

Figure 3.2: Diagram of the designed five element Yagi array antenna

3.3 Computation and Analysis of Yagi Antenna Parameters

`

This sub-section mathematically analyzed the parameters of Yagi Array antenna designed in figure 3.2 using the conventional antenna equations. The key parameters discussed here include Electric and Magnetic fields Radiated by the Antenna, Power Density or Average Poynting Vector, Radiation Intensity, Directivity, Radiation Resistance, Front to Back Ratio, and Directive Gain of the Yagi array antenna.

3.3.1 Electric and Magnetic fields Radiated by the Yagi Antenna

In the Matlab implementation, *SINTEG* function is used to analyze integration. Thus, since integration is very difficult to be analyzed here, the weighted method (Gaussian method) which states that, while resolving numerical analysis, a quadrature rule should be an approximation of the definite integral of a function, which is usually stated as a weighted sum of function values at specified points within the domain of integration was applied.

Therefore, the Electric and Magnetic fields of the Yagi Antenna array radiated at the far fields of five element Yagi array antenna in free space was obtained by summing the fields from each of the elements in the array. The far field generated by the five element yagi antenna was obtained as

$$E_\theta = \sum_{n=1}^{5} E_{\theta n} = -jwA_\theta \tag{3.42}$$

where,

$$A_\theta = \sum_{n=1}^{5} A_{\theta n} \tag{3.43}$$

This can be expressed as in (Raida and Hudak, 1997)

$$\sum_{n=1}^{5} A_{\theta n} = \frac{\mu e^{-jkr} sin\theta}{4\pi r} \sum_{n=1}^{5} \left\{ e^{jk(x_n' sin\theta cos\varphi + y_n' sin\theta sin\varphi)} \sum_{m=1}^{M} I_{nm} \left[\frac{sin(Z^+)}{Z^{\mp}} \right] + \left[\frac{sin(Z^-)}{Z^-} \right] \right\} \frac{l_n}{2} \tag{3.44}$$

`

Thus,

$$E_\theta = \frac{jk_0\eta_0 e^{-jkr}sin\theta}{4\pi r}\sum_{n=1}^{5}\left\{e^{jk(x_n'sin\theta cos\varphi + y_n'sin\theta sin\varphi)}\sum_{m=1}^{M} I_{nm}\left[\frac{sin(Z^+)}{Z^+}\right] + \left[\frac{sin(Z^-)}{Z^-}\right]\right\}\frac{l_n}{2} \quad (3.45)$$

Where

m is the mode of the current of the antenna

$$Z^+ = \left(\frac{(2m-1)\pi}{2h_n} + k_0 cos\theta\right)h_n \quad (3.46)$$

and

$$Z^- = \left(\frac{(2m-1)\pi}{2h_n} - k_0 cos\theta\right)h_n \quad (3.47)$$

where

h_n is the antenna length $l_n$divided by 2

Further analysis of the Electric field results to equation (3.48) in as much as the total radiation electric field intensity pattern of the yagi antenna is as a result of field superposition from all elements. Considering the five (5) antenna elements of the design,

$$E_\theta = \frac{j\eta_0 e^{jkr}}{2\pi r}\sum_{n=1}^{5} I_n\left(\frac{cos\left(kl_n cos\theta - cos(kl_n)\right)}{sin\theta}\right)e^{jks_{n-1}cos\theta} \quad (3.48)$$

The corresponding magnetic field is obtained thus,

$$H_\varphi = \frac{E_\theta}{\eta_0} \quad (3.49)$$

$$H_\varphi = \frac{je^{jkr}}{2\pi r}\sum_{n=1}^{5} I_n\left(\frac{cos\left(kl_n cos\theta - cos(kl_n)\right)}{sin\theta}\right)e^{jks_{n-1}cos\theta} \quad (3.50)$$

`

Given that the length of the reflector is 0.25m, dipole length of 0.22m, while the lengths of the three directors are 0.211m, 0.202 and 0.193 respectively. Also, the spacings of 0.108m between reflector and dipole, 0.086m between dipole and first director, 0.069m between first director and second director, and then 0.052m between second director and third director, with dipole wavelength of 0.43m, the Electric and Magnetic fields of the yagi antenna was plotted using MatLab software.

The detailed derivation of the Electric and Magnetic fields is shown in Appendix C.

3.3.2 Power Density or Average Poynting Vector

The Power density or Average poynting vector of the Yagi array antenna is obtained from the relation in equation (3.51) (Balanis, 2005)

$$\rho_{ave} = \frac{1}{2} Re\left(E_\theta \times H_\varphi^*\right) \tag{3.51}$$

Substituting equations (3.31) and (3.33) into equation (3.34) results to equation (3.52)

$$\rho_{ave} = \frac{\eta_0}{8\pi^2 r^2}\left\{\sum_{n=1}^{5} I_n \left(\frac{cos\left(kl_n cos\theta - cos(kl_n)\right)}{sin\theta}\right) e^{jks_{n-1}cos\theta}\right\}^2 \bar{a}_r \tag{3.52}$$

The plot of the average pointing vector was simulated at the reflector length of 0.25m and dipole length of 0.22m. The lengths of the three directors were 0.211m, 0.202m and 0.193m respectively.

In order to obtain total Power (P) radiated by the antenna, equation (3.44) $\rho_{ave} ds$ was integrated over a closed sphere of radius 'r' such that; (Agnihotri, Prabhu and Mishra, 2013).

`

$$\rho_{ave} = \frac{\eta_0}{8\pi^2 r^2}\int_0^{\pi}\int_0^{2\pi}\left\{\sum_{n=1}^{5} I_n\left(\frac{cos(kl_n cos\theta - cos(kl_n))}{sin\theta}\right)e^{jks_{n-1}cos\theta}\right\}^2 sin^3\theta d\theta d\varphi \quad (3.53)$$

3.3.3 Radiation Intensity

Radiation intensity $U(\theta,\varphi)$ is represented as the product of square of the distance from origin to the far field point denoted by 'r' and the average poynting vector. This is shown in equation (3.54) (Balanis, 2005)

$$U(\theta,\varphi) = \rho_{ave} \times r^2 \quad (3.54)$$

Resolving equation (3.54) results to equation (3.55)

$$U(\theta,\varphi) = \frac{\eta_0}{8\pi^2 r^2}\left\{\sum_{n=1}^{5} I_{nm}\left(\frac{cos(kl_n cos\theta - cos(kl_n))}{sin\theta}\right)e^{jks_{n-1}cos\theta}\right\}^2 \bar{a}_r \times r^2 \quad (3.55)$$

Which then becomes,

$$U(\theta,\varphi) = \frac{\eta_0}{8\pi^2}\left\{\sum_{n=1}^{5} I_n\left(\frac{cos(kl_n cos\theta - cos(kl_n))}{sin\theta}\right)e^{jks_{n-1}cos\theta}\right\}^2 \bar{a}_r \quad (3.56)$$

The radiation intensity was then simulated with the MatLab software.

3.3.4 Directivity

Directivity is the ratio of maximum radiation intensity from an antenna (power per unit solid angle) $U(\theta,\varphi)_{\max}$ to the average radiation intensity U_{av} (averaged over a sphere)(Kraus,1988). Directivity of an antenna is also defined as the maximum value of its directive gain. It is determined thus,

$$D_{max} = \frac{4\,\pi\, U_{max}}{P_{rad}} \quad (3.57)$$

$$D_{max} = 1.5 \sin\theta \quad (3.58)$$

$$D_{max} = 1.5 \quad (3.59)$$

`

This occurs at ɵ = 90 ^{0}

Hence, the Directivity of a five-element yagi array antennas was calculated and plotted. The yagi array directivity was computed as a product of equation (3.58) and conventional array factor (AF). The MatLab programmes for the computation were shown in Appendix G and Appendix H respectively.

3.3.5 Radiation Resistance

Radiation resistance of an antenna is expressed as,

$$R_{rad} = \frac{2P}{I^2} \tag{3. 60}$$

where

I is the current at the driven element ,

R_{rad} is the radiation resistance in ohms and

P is the total Power radiated by the antenna.

Radiation resistance of an antenna is important in order to ensure easy match of transmission line to the feed point in order to prevent power losses.

3.3.6 Directive Gain, D (ɵ, φ):

Directive Gain is the ratio of antenna radiation intensity to that of a hypothetical isotropic radiator that radiates the same power. (Balanis, 2005)

$$\mathrm{D}(\theta, \varphi) = \frac{\mathrm{U}(\theta,\varphi);}{U_0} = \frac{4\,\pi\,\mathrm{U}(\theta,\varphi)}{P_{rad}} \tag{3.61}$$

$$\mathrm{D}(\theta, \varphi) = 1.5 \sin^2\theta \tag{3.62}$$

The yagi array directivity was also computed as a product of equation (3.62) and array factor (AF). The MatLab programmes for the computation were shown in Appendix I and Appendix J respectively.

`

Matrix Laboratory (MatLab) Software Tool

The collected data as well as the antenna parameters were analyzed by Matlab (MATLAB R2010a) software tools. The choice of the MatLab software was made because it possesses user friendly built-in tools and prevailing advantages in behaviour analysis; it has an interactive platform for calculation, visualization, and programming; it minimizes the complexity of data analysis and applications creation; MatLab built-in *Math Functions* allow for investigation of multiple approaches. These benefits are derivable from it as compared to other simulation software tools.

`

CHAPTER FOUR
RESULTS AND DISCUSSIONS

4.1 RESULTS

In this chapter, the data calculated as tabulated in Table 3.5 for the antenna parameters were analyzed and plotted using Matlab software tools. The antenna array current generated from the use of MoM as represented in Appendix B was employed in the analysis. Thus, five (5) sets of results were presented, namely:

i. the Cartesian and polar plots of the Electric/Magnetic Fields of the Yagi antenna;
ii. the polar plot of the Average Poynting Vector of the Yagi antenna;
iii. polar plot of the Radiation Intensity of the antenna;
iv. polar plot of the antenna directivity and;
v. the polar plot of the Directive Gain of the yagi antenna

The antenna structure comprises five (5) elements (a reflector, a dipole, and three (3) directors).

These results were plotted at an intrinsic impedance of 377Ω; a far field distance of 50m (distance from the antenna source point to the far field point); and antenna wave number of 1.

Electric and Magnetic (E and H) Fields of the Yagi Antenna

`

Figure 4.1 shows the Cartesian plot of Electric and Magnetic fields of the Yagi Antenna.

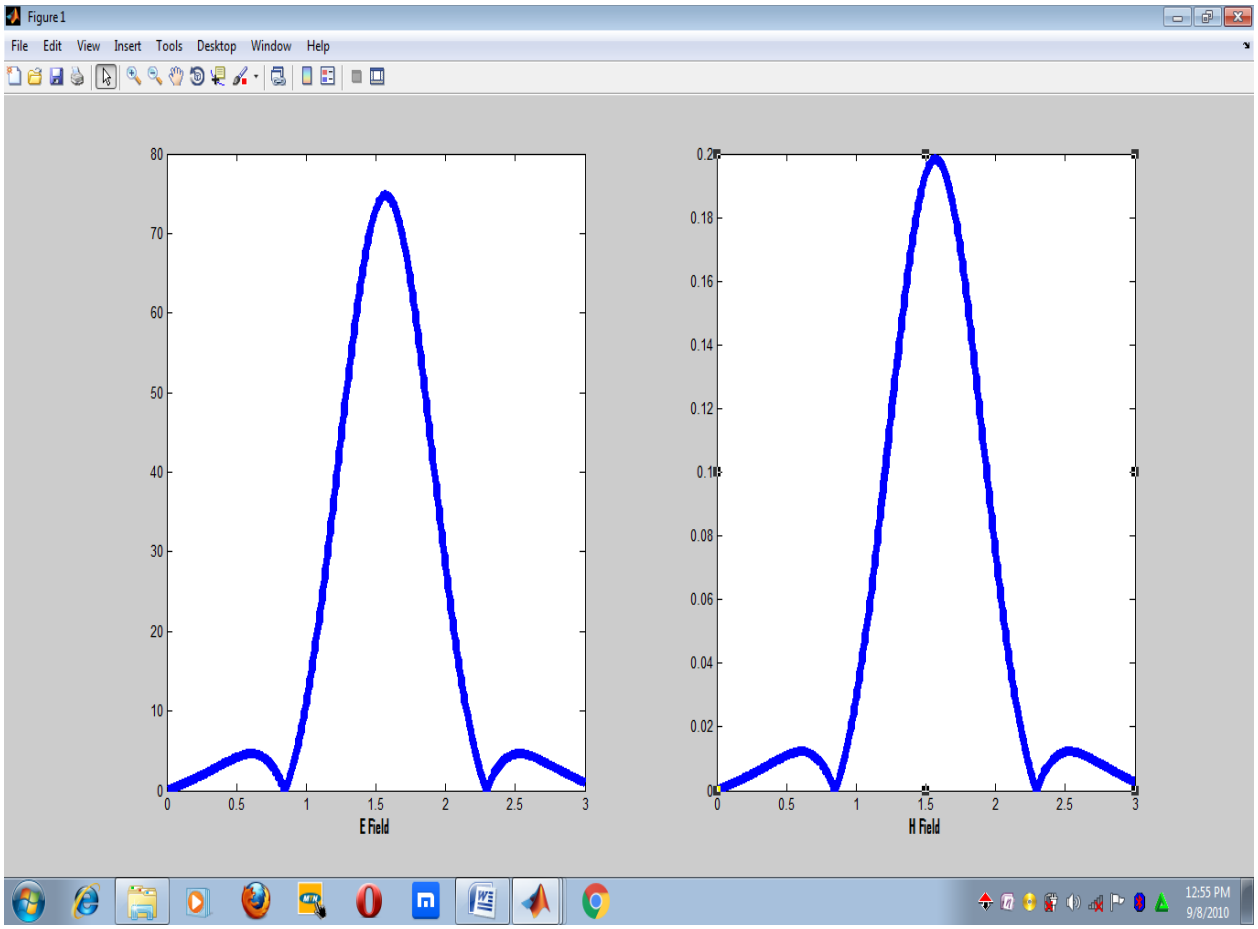

Figure 4.1: Cartesian plot of Electric and Magnetic fields of the Yagi Antenna

Figures 4.1 shows the radiated Electric and Magnetic fields generated from the simulation of the designed yagi antenna respectively. Caution was taken in choosing the angle within which the fields were radiated in order to ensure that the generation of repeated lobes was avoided. Otherwise, this normally has adverse effect of not only subtracting from the total radiated power, but also

`

affects the operators behind the transmitting system (Kouzmanova, Atanasova, Atanasov, and Tasheva, 2007).

Figure 4.2 demonstrates the polar plot of the Electric Field and the corresponding Magnetic Field of the same yagi antenna as represented in the experimental antenna respectively.

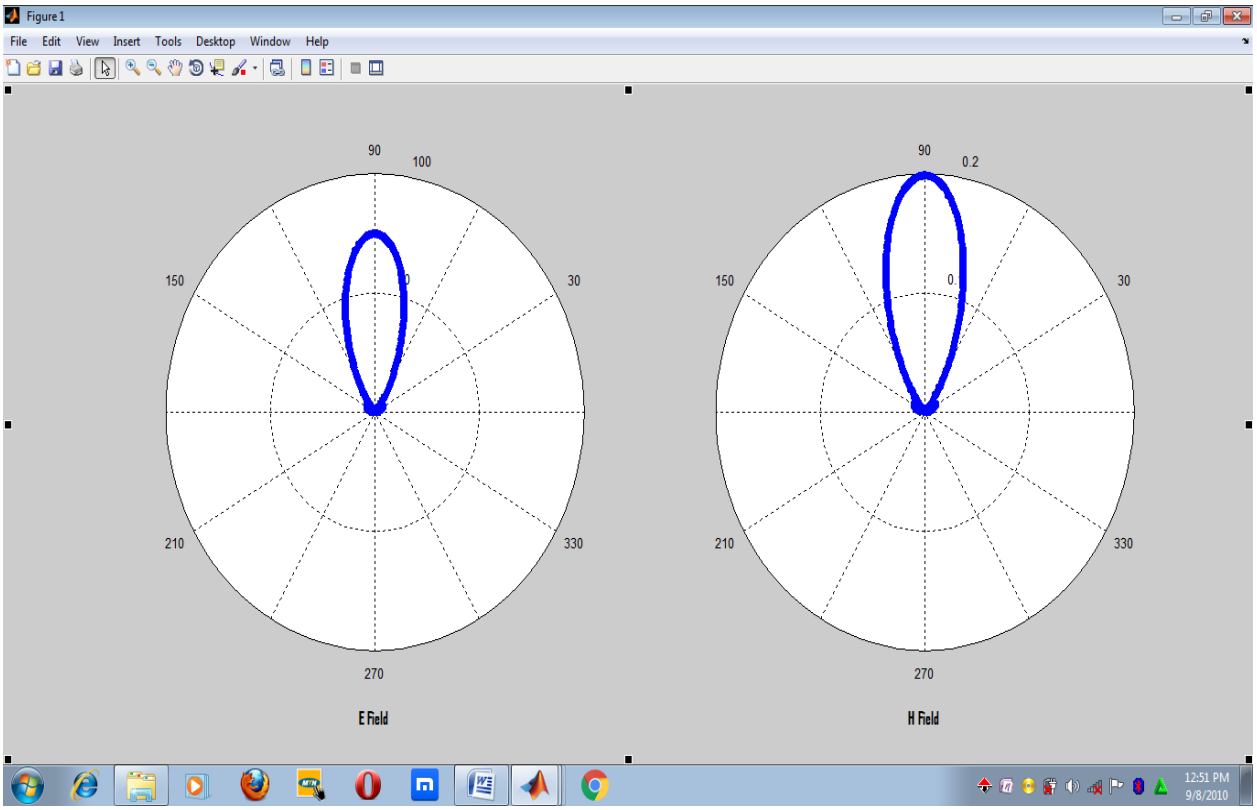

Figure 4.2: Polar plot of Electric and Magnetic fields of the Yagi Antenna

It could be keenly observed that both field patterns are similar in shape except that the Electric field is of higher magnitude. The magnetic field as in equation

`

(3.50) was obtained by dividing the electric field of equation (3.48) by the intrinsic impedance, 120π.

Average Poynting Vector of the Yagi Antenna

Figure 4.3 shows the polar plot of Average poynting Vector of the Yagi Antenna.

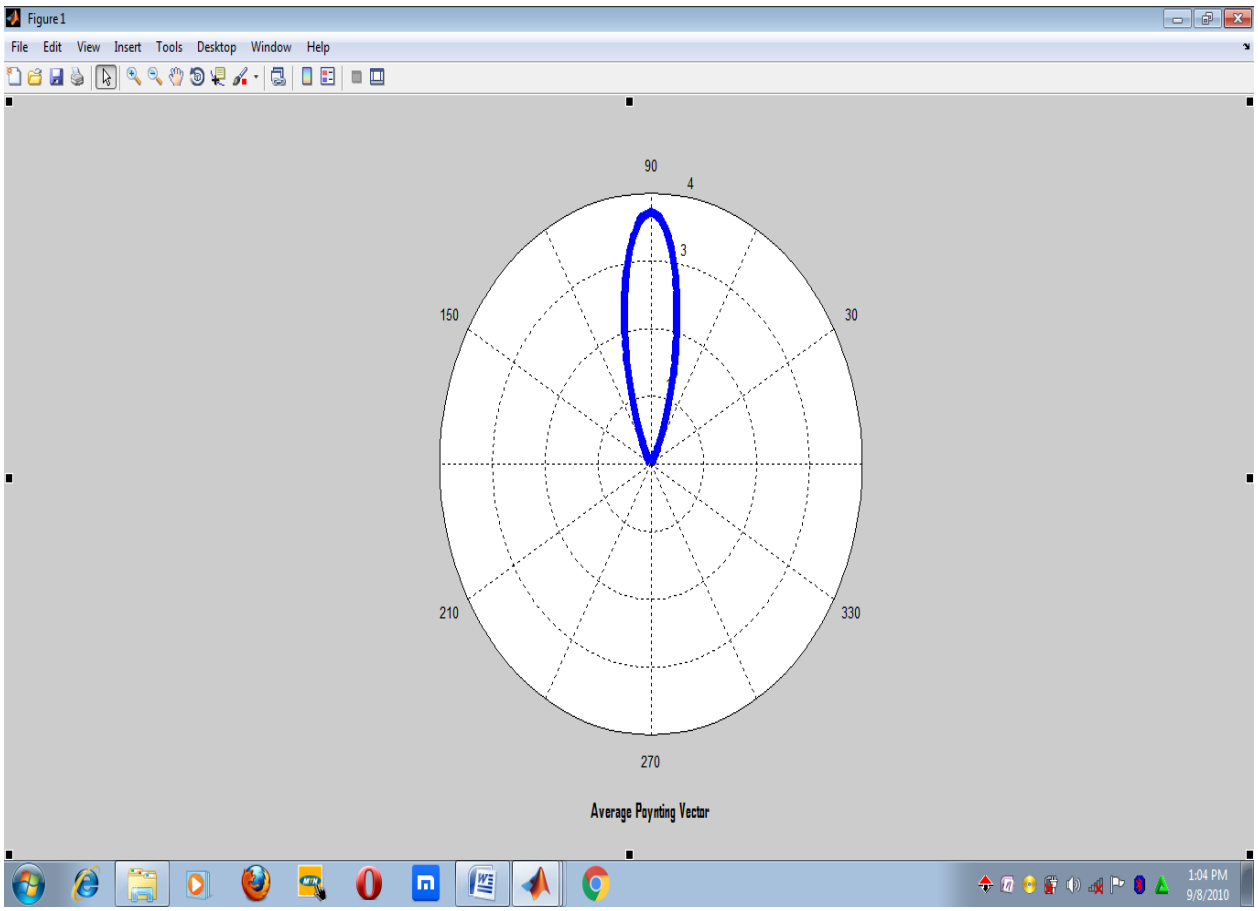

Figure 4.3: Polar plot of Average poynting Vector of the Yagi Antenna

`

The Average poynting Vector of the Yagi Antenna was obtained from the average value of the vectorial product (of the real values) of the Electric and Magnetic fields of the Yagi Antenna. This is as denoted in equation (3.52).

Radiation Intensity of the Yagi Antenna

Figure 4.4 illustrates the Radiation intensity of the Yagi Antenna .

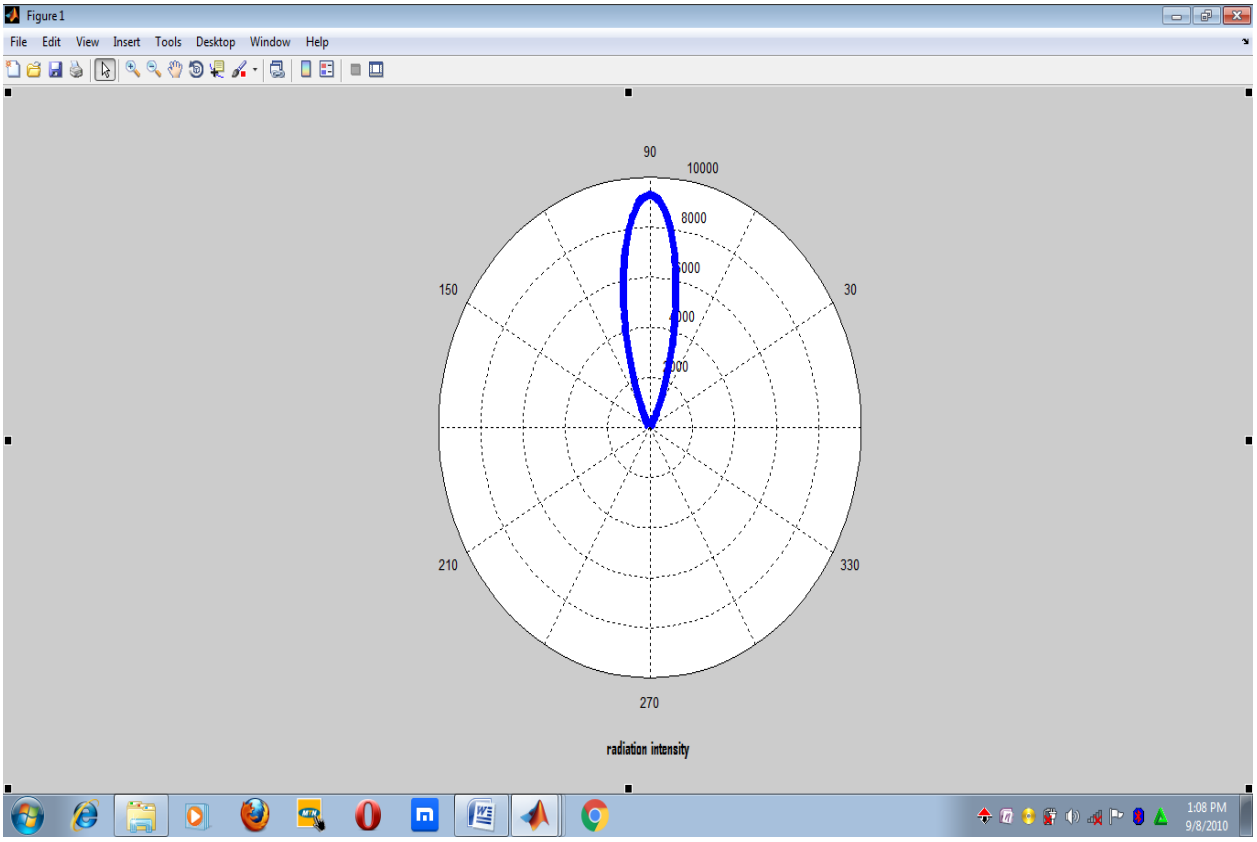

Figure 4.4: Polar plot of Radiation intensity of the Yagi Antenna

The plot of the Radiation Intensity of the designed Yagi Antenna was obtained using equation (3.56). The plot was obtained as a product of the average

`

poynting vector and square of the distance from the yagi antenna origin to the far field point denoted by ‘r’.

Directivity of the Yagi Antenna

The polar plot of directivity of Yagi array Antenna was plotted and shown in Figure 4.5.

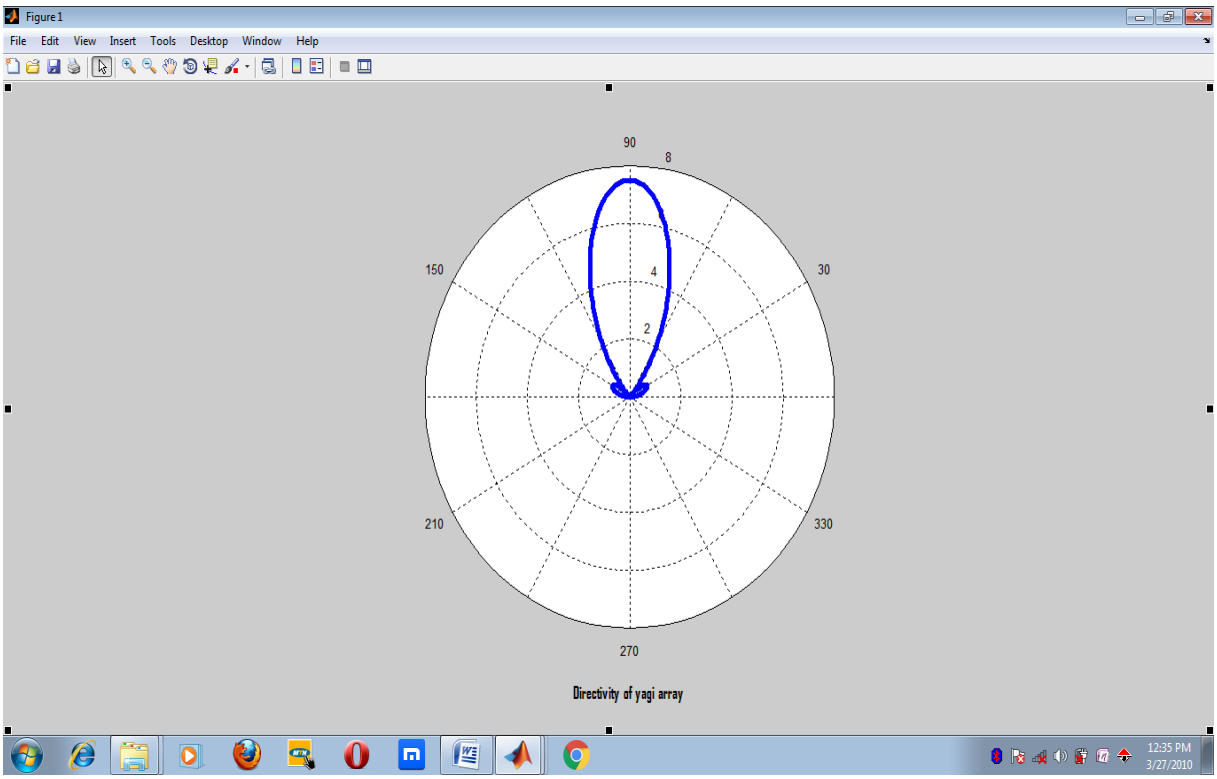

Figure 4.5: Polar plot of Directivity of the Yagi Antenna

`

In Figure 4.5, directivity of the yagi antenna was very directive in nature. This was true as directivity is the ratio of maximum radiation intensity from an antenna (power per unit solid angle) to the average radiation intensity.

Directive Gain of the Yagi Antenna

Figure 4.6 represents the polar plot of the directive gain of the Yagi Antenna.

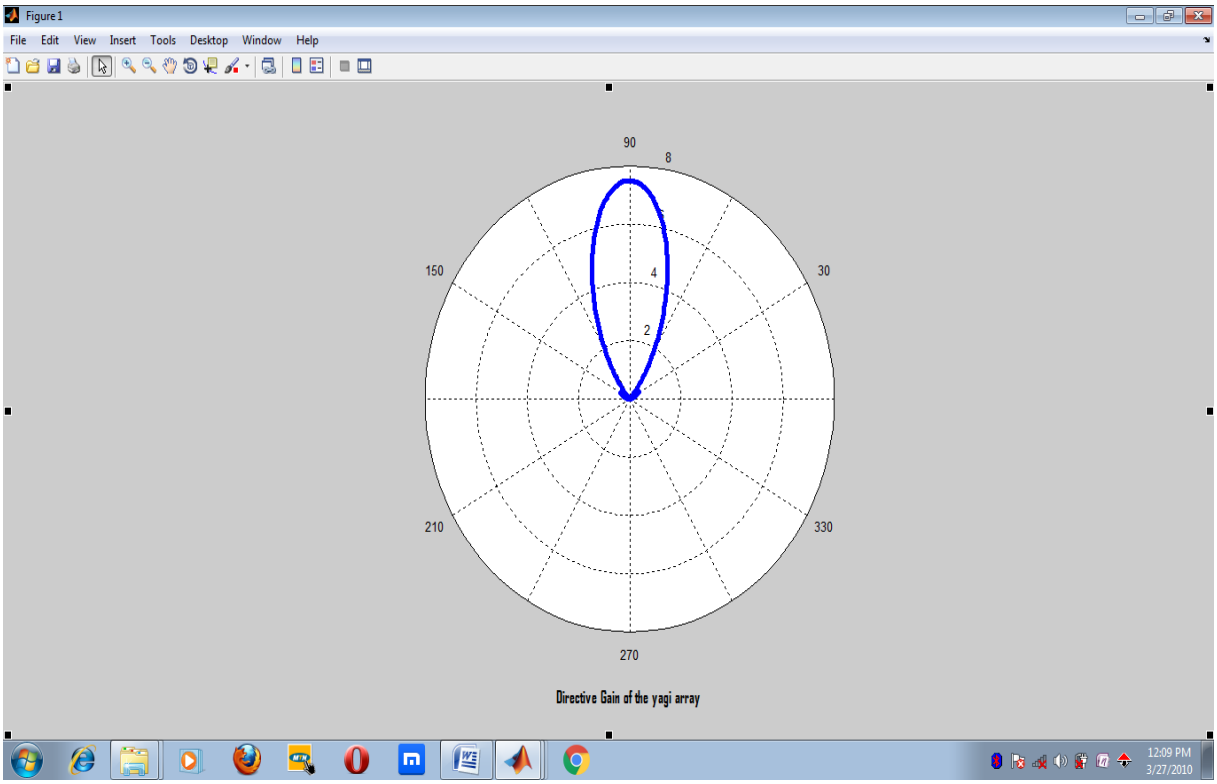

Figure 4.6: Polar plot of Directive Gain of the Yagi Antenna

`

Figure 4.6 represents the directive gain of Yagi Antenna. From the design, the signals were radiated within the angle of π. The plot of the Directive gain of the yagi antenna was developed from equation (3.62) by multiplying the directivity of the antenna by the square of the sine of the radiation angle, Θ.

4.2 DISCUSSION

Figure 4.1 denotes the radiated Electric and Magnetic fields generated from the simulation of the designed yagi antenna respectively. The generated lobes of Figures 4.1 were directional with minimal sidelobes. This helped in focusing the radiated signal in the direction of interest. Also, because the radiation pattern was directive, there were little chances for the detection of unwanted signals around the signal of interest. Hence, this improved the precision for the performance of the yagi antenna array.

In figure 4.2, the magnetic field as in equation (3.50) was obtained by dividing the electric field of equation (3.48) by the intrinsic impedance, 120π. Hence, the magnitude of the pattern of the magnetic field was decreased as witnessed in the figure 4.2. While the Electric field is having a magnitude of about 75 Newtons/coulomb (as can be viewed from the plot), the magnetic field is having a magnitude of 0.2 Tesla, as could be read from the plot. These values were very appropriate when compared to other directional antennas like Log-periodic dipole array antenna, as earlier reviewed.

`

Figure 4.3 denotes the average poynting vector of the designed yagi antenna. From the plot, the average pointing vector was 3.73 watt per square metre as read from the antenna pattern. Thus, the implication of this was that the power density of 3.73 watt was concentrated within the direction of the radiated signal of interest. This influenced the distance the radiated signal could travel.

From figure 4.4, the radiation intensity of the yagi antenna was obtained as a product of the average poynting vector and square of the distance from the yagi antenna origin to the far field point denoted by 'r'. The radiation intensity pattern was very directive and of higher magnitude compared to the Average poynting Vector of the same antenna. Keen observation of the antenna pattern indicated that the Yagi antenna has a Radiation Intensity value of about 9.400 c/kg.

Observing figure 4.5, the directivity of the yagi antenna of figure 4.5 was very directive. This was true as directivity is the ratio of maximum radiation intensity from an antenna (power per unit solid angle) to the average radiation intensity. From the graph, the directivity of the yagi array antenna was about 9.03 dBi (That is: 10 Log 8).Thus, the yagi array has an average directivity of about 9 dBi which is far better than that of the equivalent log-periodic dipole antenna array of 6.5dBi.

Figure 4.6 represents the directive gain of Yagi Antenna. The yagi array directive gain was equivalent to its directivity (9dBi). Hence, the yagi antenna showed a higher directive gain compared to most array antennas like log-

`

periodic dipole antennas of about 6.5 dBi, and even greater than that obtained for dipole antennas (1.76dBi). This was very beneficial to direction finding system application. It has a high antenna gain which enables the generated signal travel a longer distance as well as eliminates detection of clutters within the target area.

CHAPTER FIVE

CONCLUSIONS AND RECOMMENDATIONS

5.1 CONCLUSIONS

In this thesis, the performance of direction finding system antenna was improved by generating the approximate current distribution for a direction finding system antenna via Method of Moment approach. An experimental Yagi antenna was designed and analyzed for the study. The antenna had a single reflector, one active (driven) element and three parasitic directors.

The parameters of the Yagi antenna of the direction finding system were numerically developed and analyzed at far field of the antenna using Magnetic Vector Potential (MVP) technique. This antenna was designed and operated at an Ultra High Frequency band of 0.6GHz – 0.8GHz, wave number of one (1), intrinsic impedance of 377Ω. The measurement was carried out at a distance of 50m from the antenna source to the far field of the Yagi antenna.

Afterwards, the MatLab software tools were used to simulate the antenna Electric/Magnetic fields and other parameters of the antenna which included the Average poynting Vector, Radiation Intensity, the directivity as well as the directive gain of the Yagi antenna.

`

The results from the analyzed Yagi antenna indicated an appreciable and improved directivity of 9.03dBi compared to that of log-periodic antenna of 6.5 dBi.

5.2 RECOMMENDATIONS:

The outcome of this research should be beneficial to both stakeholders in antenna engineering and for surveillance applications. Thus, to further improve on the performance of the direction finding systems antenna, the following are recommended.

i. To increase the directionality of the yagi antenna, the antenna designers could add elements to the yagi antenna array. The antenna essentially becomes narrower in its focus, but it then detects signals from that direction even better than before. This is because of an improved signal to noise ratio. Thus, the interference levels would be reduced, especially from the sides.

ii. It is also recommended that circular elements be used in place of the linear elements in analyzing the parameters of the yagi antenna for the direction finding system using same moment method approach. This approach will drastically minimize the physical dimensions of the antenna.

5.3 CONTRIBUTIONS TO KNOWLEDGE

`

i. The work developed an approach for the system designers to generate an approximate current distribution for a direction finding system antenna which helps to minimize the detection of false alarms by the DF system. This assists in forecasting the exact performance of direction finding system prior to costly prototype development and deployment.

ii. The combination of the Moment Method with the Magnetic Vector Potential operator in the analysis of the yagi antenna array not only improved the precision of the current, but also reduced the antenna current computation time.

iii. The computed antenna parameters very precise as it was computed with the approximate current generated from the Moment Method, and thus improved the directivity of the yagi antenna array pattern.

`

REFERENCES

Abbosh, A. (2012). Design and Analysis of Wideband Passive Microwave Devices Using Planar Structures. PhD Dissertation. Published Works Submitted To The Faculty Of Engineering, Architecture And Information Technology, The University Of Queensland, Australia.

Adekola, S. A. and Raji, A. A. (2017). Comparative Performance Characteristics of Yagi- Uda Arrays of Uniform and Varying Lengths of Directors with Uniform and Parabolic Spacings. 2017 IEEE 3rd International Conference on Electro-Technology for National Development (NIGERCON), pp 211 – 219.

Agnihotri , A., Prabhu , A. and Mishra, D. (2013). Improvement in Radiation Pattern Of Yagi-Uda Antenna. *Research Inventy: International Journal Of Engineering And Science Vol.2, Issue 12, Pp 26-35*

Alexander, W. C. (2012). AM Antenna Computer Modeling: A Tutorial on Moment Method Computer Modeling for Performance Verification of AM Directional Arrays. Crawford Broadcasting Company.

Asianuba. I.B., Nzeako, A.N., Sapre-Obi, E. (2014). Method of Moments for Antenna Analysis. Int. Journal of Applied Sciences and Engineering Research, Vol. 3, Issue 1, pp 32 – 38.

`

Balanis, C. A., (2005). “Antenna Theory Analysis and Design”. *A John Wiley & sons Inc. Publication*, 3rd Edition.

Cicchetti, R., Miozzi, E. and Testa, O. (2017). “Wideband and UWB Antennas for Wireless Applications: A Comprehensive Review,” International Journal of Antennas and Propagation, vol. 2017, Article ID 2390808, 45 pages, 2017. doi:10.1155/2017/2390808

Collin, R. E. (1985). “Antennas and Radiowave Propagation”. *International student ed.* New York: McGraw-Hill.

Collin, R. E. (2001). “Foundations for Microwave Engineering”. *A john wiley and sons, inc publication.* 2nd edition. New York: McGraw-Hill.

Dhande, P. (2009). “Antennas and its Applications. DRDO Science Spectrum”. Pp 66-78.

Douglas, S. (2014), 4G Wireless Communications: Real World Aspects and Tools. Intel Technology Journal, Vol. 18, Issue 3.

“EffectiveAperture”Source:http://elearningatria.files.wordpress.com/2013/10/ece-vi-antennas-and-propagation-10ec64-notes.pdf

Ena, (2012). “ Electric and Magnetic Fields” produced by Energy Networks Association.

`

Federal Communications Commission (2009). Media Bureau Clarifies Procedures For Am Directional Antenna Performance Verification Using Moment Method Modeling, pg 1 – 4.

Gladwin, Lee A. (1997). Alan Turing, Enigma, and the Breaking of german Machine Ciphers in World War II, Prologue, pp 203 – 217.

Guerin, D., Jackson, S. and Kelly, J. (2012). Passive Direction Finding: A Phase Interferometry Direction Finding System for an Airborne Platform. A Project submitted to the faculty of Worcester Polytechnic Institute.

Healy, J. W. (1991) " Antenna, Here is a dipole ". http://hraunfoss.fcc.gov/edocs_public/attachmatch/DA-09-2340A1.pdf

Jun-Ho, C., Joon-Ho, S., Cheol-Sun, P. and Seung-Sub, O. (2006). Active Composite Dipole Antenna for Direction Finding Array Antenna Applications. Conference Paper: *IEEE Xplore*, August 2006, pp 1153 – 1156.

Khan, Riaz and bilal (2016). " Various types of Antenna with respect to their Applications" : International journal of Multidisciplinary Sciences and Engineering, Vol.7, No.3, March 2016.

Kouzmanova, M., Atanasova, G., Atanasov, N. and Tasheva, S. (2007). Effects of in vitro exposure to GSM900 electromagnetic field on human erythrocytes. The Environmentalist, Volume 27, Issue 4, pp 423–428.

Kraus, J. D. (1997). "Antennas For all Applications". *Tata McGraw-Hill publishing company Ltd*, New Delhi, 2nd Edition.

Kraus, J. D., and Marhefka, R. J. (2001). *Antennas for all Applications.* 3rd Edition.

`

Kshetrimayum, R.S, (2016). " Electromagnetic Field Theory"

Lingel,S. Rhodes, C., Cordova, A., Hagen, J., Kvitky, J. and Menthe, L. (2008). Methodology for Improving the Planning, Execution, and Assessment of Intelligence, Surveillance, and Reconnaissance Operations. Technical Report Prepared for the United States Air Force, Approved for public release.

McDonald, K. T. (2009). Currents in a Center-Fed Linear Dipole Antenna. Joseph Henry Laboratories, Princeton University, Princeton, NJ 08544,pp 1 – 20.

Mohammad, S. S. and Daniel, N. A. (2011). Design of an 8-element switched mode circular antenna array for vehicular direction finding, Conference: *Wireless and Microwave Technology Conference* (WAMICON), 2011 IEEE 12th Annual, pg 1 – 4.

Neelakanta, S.P., & Chatterjee, R. (2003). "Antennas for Information Super Skyways: An Exposition on Outdoor and Indoor wireless Antennas". *Research Studies Press Ltd*, England.

Ozec, M. O. (2011). Direction Finding Performance Of Antenna Arrays On Complex Platforms Using Numerical Electromagnetic Simulation Tools. A thesis submitted to Electrical and Electronics Engineering Department, Middle East Technical University.

Patidar, D., Singhal, P.K., Gupta, H. K. and Prjapati, R. (2012). Design & Investigation of Five Element Liquid Yagi Uda Antenna at L-Band(1 GHz) Applications. *International Journal of Engineering and Technology, 1 (3), pp 250-255*

`

Rahim, T. (2015). An Overview of Helix Antenna and Its Design. ResearchGate. pp 1 – 17. https://www.researchgate.net/publication/272348908

Raida and Hudak, (1997). " Analysis of Wire Antennas by Moment Methods" Radioengineering Vol.6, No.2, June 1997.

Raida, Z. and Hudak, I. (1997). Analysis of Wire Antennas by Moment Methods. Radioengineering, Vol. 6, No. 2, pp 1 – 8.

Ranga, R. (2010). ''Fundamental Parameters of Antenna''.

Rao, K., Singh, A.K. and Singh, S. P. (2014).Novel Design and Implementation of Base Line Interferometry Direction Finding Bli Df Algorithm. SSRG International Journal of Electronics and Communication Engineering (SSRG-IJECE) – volume 1, issue8, pp 14 – 19.

Rohde and Schwar (2015). "Antenna Basics". http://cdn.rohde-schwarz.com/pws/dl_downloads/dl_application/application_notes/8ge01/Antenna_Basics_8GE01_1e.pdf. Pp 1-32.

Sarkar, T. K., Djordjevic, A. R., and Kolundzija, B. M. (2000). Method of Moments Applied to Antennas. Department of Electrical and Computer Engineering, Syracuse University, N.Y. 13244-1240, USA.

Segun, A. A., Olasope, A. M., Okeowo, R. C. and Ismail, A. A. (2013). Design And Numerical Analysis Of A Single Half-Wave Dipole Antenna Transmitting At 235MHz Using Method Of Moment. IJRRAS, Vol. 15, Issue 1, pp 107 – 119.

Shi, H. (2014). Physical-Layer Communications Using Direct Antenna Modulation. A Thesis Submitted To the Department of Electronic and Electrical Engineering the University Of Sheffield for the Degree of

`

Doctor of Philosophy

Singh, S. K., Solanki, P. and Solanki, R. (2014). "Introduction to Antenna, their Types and their Application". *International Journal of Innovative Research in Technology*: volume 1, Issue 6, pp 1574 – 1577.

Sinha, S. N. (2017). A Brief History of Microwave Engineering. Dept. Of Electronics & Computer Engineering IIT Roorkee, pg 1 – 50.

Staelin, D. H. (2011). Electromagnetics and Applications. Department of Electrical Engineering and Computer Science Massachusetts Institute of Technology Cambridge, MA.

Taylor, J. and Huang, Q. (1997). CRC Handbook of Electrical Filters. CRC Press, New York.

Warnick, K. F. (2014). Ultra-high Efficiency Phased Arrays for Astronomy and Satellite Communications. Department of Electrical and Computer Engineering Brigham Young University, Provo, UT, USA. pp 64.

Weldon, J. A. (2010). A Direction Finding System Using Log Periodic Dipole Antennas In A Sparsely Sampled Linear Array. Msc Thesis, Department of Electrical Engineering, Wright State University.

Xie, Y., Fan, X., Wilson, J. D., Simons, R. N., Chen, Y. and& Xiao, J. Q. (2014). A Universal Electromagnetic Energy Conversion Adapter Based On A Metamaterial Absorber. Department of Electrical and Electronic Engineering.

Yang, ChenNing (2014). "The conceptual origins of Maxwell's equations and gauge theory". Physics Today. **67** (11): 45–51.

`

Zhang, J., Tian, G. Y., Marindra, A. M. J., Sunny, A. I., & Zhao, A. B. (2017). A Review of Passive RFID Tag Antenna-Based Sensors and Systems for Structural Health Monitoring Applications. *Sensors (Basel, Switzerland)*, *17*(2), 265. http://doi.org/10.3390/s17020265

Appendix A

Given that the approximated current is as shown in equation (1)

$$I_n(z_n') = \sum_{m=1}^{M} I_{nm} cos\left[\frac{(2m-1)\pi z_n'}{2\left(\frac{l}{2}\right)_n}\right], \text{m} = 1,2,3 \ldots\ldots \text{M} \quad (1)$$

When equation (1) of the complex current coefficient is substituted into equation (2),

$$(z) =$$

$$\frac{\eta_0}{jk_0} \sum_{n=1}^{N} \int_{-\frac{l_n}{2}}^{+\frac{l_n}{2}} I_n(z_n') \left\{ [(1 + jk_0R)(2R^2 - 3a^2) + k_0^2R^2a^2] \frac{e^{-jk_0R}}{4\pi R^5} dz_n' \right\} \quad (2)$$

we then have

$$E^i(z) = \frac{j\eta_0}{k_0} \sum_{n=1}^{N} \sum_{m=1}^{M} I_{nm} \int_{-\frac{l_n}{2}}^{+\frac{l_n}{2}} cos\left[\frac{(2m-1)\pi z_n'}{2\frac{l_n}{2}}\right] \left[(1 + jk_0R_n)\left(2{R_n}^2 - 3a^2\right) + k_0^2{R_n}^2a^2\right] \frac{e^{-jk_0R_n}}{4\pi R_n^5} dz_n' \quad (3)$$

`

Applying the Dirac delta function on equation (3),

$w_p(z) = \delta(z - z_p)$

where,

$p = 1, 2.....M$,

z_p is the discrete point where the boundary condition is implemented.

The Dirac function will be employed as weighting function. Its inner product is taken with equation (3) which results to equation (4)

$$\int_{-\frac{l}{2}}^{+\frac{l}{2}} w_p(z)E^i(z)dz = \frac{j\eta_0}{k_0} \sum_{n=1}^{N} \sum_{m=1}^{M} I_{nm} \int_{-\frac{l_n}{2}}^{+\frac{l_n}{2}} w_p(z)\ cos\left[\frac{(2m-1)\pi z_n'}{2\frac{l_n}{2}}\right] \left[(1 + jk_0R_n)\left(2{R_n}^2 - 3a^2\right) + k_0^2{R_n}^2a^2\right] \frac{e^{-jk_0R_n}}{4\pi R_n^5} dz_n'\, dz \quad (4)$$

Equation (4) reduces to (5) since the integral of any function multiplied by $\delta(z - z_p)$ gives the value of the function at z = z_p,

$$\int_{-\frac{l}{2}}^{+\frac{l}{2}} w_p E^i(z)dz = \frac{j\eta_0}{k_0} \sum_{n=1}^{N} \sum_{m=1}^{M} I_{nm} \int_{-\frac{l_n}{2}}^{+\frac{l_n}{2}} cos\left[\frac{(2m-1)\pi z_n'}{2\frac{l_n}{2}}\right] \left[(1 + jk_0R_{np})\left(2R_{np}^2 - 3a^2\right) + k_0^2R_{np}^2\, a^2\right] \frac{e^{-jk_0R_n}}{4\pi R_{np}^5} dz_n' \quad (5)$$

where

$R_{np} = \sqrt{a^2 + \left(z_p - z_n'\right)^2}$

Changing equation (5) into the conventional impedance matrix equation, we obtain equation of the form represented in equation (6)

$[V] = [I][Z]$ (6)

where,

V is the voltage matrix (This represents entries that account for antenna's excitation as a result of the impressed field,

`

I is the unknown current coefficient and,

Z is the impedance matrix (It is made of elements formed by the inner product of testing function with integral on basis function.

The antenna elements are divided into M segment modes. The feed on the driven element was modeled by Delta-gap model with a feed voltage of 1Volt. Also, the entries into voltage matrix are zeros except at the feedpoint.

Hence, the system of matrix equations was then solved to find the complex coefficient of the current distribution on each wire by finding the product of the voltage matrix and the inverse of an impedance matrix as represented in equation (7).

$$[I] = [V]\left[\frac{1}{Z}\right] \quad (7)$$

Equation (5) was implemented with the aid of matlab simulation code of Appendix B.

`

Appendix B

```
% Matlab plot of the current value from Moment method of Yagi uda antennas
% for Direction Finding System

p=zeros(1,5);
f1=zeros(1,5);
k_0=1;
zp=6;
z_n=1;
a=10;
R_np=sqrt(a^2+(zp-z_n)^2);
m=1;
intimp=377;

syms p real double
leng=[0.25,0.22,0.211,0.202,0.193];
   s=((1+j*k_0*R_np).*((2*R_np^2)-(3*a^2) )+(k_0^2*R_np^2*a^2));
```

```
`
   k=(exp(-j*k_0* R_np)./(4*pi*R_np^5));

   f=s*k;

   i = 1;
   sum = 0;

 for s1=1:1:5

   leng(s1)= (cos((2*m-1)*pi*z_n)/(2*(leng(s1)/2)));

   p(s1)= f*leng(s1);

   f1 = int (p(s1));

   while i <= s1;
   sum=sum+f1;
   i = i + 1;
   end;

end;

curre=(sum.*(j*intimp)./k_0)./R_np;
disp(R_np)
disp(curre)
```

`

pretty(curre)

Appendix C

The Magnetic Vector Potential of the array is expressed as

$$A_\theta = \sum_{n=1}^{N} A_{\theta n} \tag{1}$$

$$A_{\theta n} = -\frac{\mu_0 \sin\theta}{4\pi} \int_{-h_n}^{h_n} I_n\left(z_n'\right) \frac{e^{-jk_0 R}}{4\pi R} dz_n' \tag{2}$$

$$R = \left|r - r'\right| \cong r \quad \text{(Amplitude approximation)} \tag{3}$$

$$R = \left|\bar{r} - \bar{r}'\right| \cong \bar{r} - \bar{r}.\bar{r}' = \mathrm{r} - \left(x'\cos\varphi\sin\theta + \mathrm{y}'\sin\varphi\sin\theta + \mathrm{z}'\cos\theta\right) \text{ (phase approximation)} \tag{4}$$

Using equation 3in the denominator of $\exp^{\left(-jk_0R\right)/R}$ and 4 in the numerator of $\exp^{\left(-jk_0R\right)/R}$ as well, we have

$$A_{\theta n} = \frac{-\mu_0 e^{-jk_0 r}\sin\theta}{4\pi r} \int_{-h_n}^{h_n} I_n\left(z_n'\right) e^{jk_0\left(x_n'\sin\theta\cos\varphi + y_n'\sin\theta\sin\varphi + z_n'\cos\theta\right)} dz_n' \tag{5}$$

$$A_{\theta n} = \frac{-\mu_0 e^{-jk_0 r}\sin\theta}{4\pi r} e^{jk_0\left(x_n'\sin\theta\cos\varphi + y_n'\sin\theta\sin\varphi\right)} \int_{-h_n}^{h_n} I_n\left(z_n'\right) e^{jk_0 z_n'\cos\theta} dz_n' \tag{6}$$

`

x_n', y_n' represent the positions on the nth element.

The E-theta component of the fields radiated by the nth element antenna is expressed as

$$E_\theta = -j\omega A_\theta \tag{7}$$

$$A_\theta = \sum_{n=1}^{N} A_{\theta n} = \frac{-\mu_0 e^{-jk_0 r}\sin\theta}{4\pi r}\sum_{n=1}^{N}\left\{ e^{jk_0\left(x_n'\sin\theta\cos\varphi + y_n'\sin\theta\sin\varphi\right)} \int_{-h_n}^{h_n} I_n\left(z_n'\right) e^{jk_0 z_n'\cos\theta} dz_n' \right\} \tag{8}$$

Using equation 8 in 7, we have

$$E_\theta = \frac{j\omega\mu_0 e^{-jk_0 r}}{4\pi r}\sum_{n=1}^{N}\left\{ e^{jk_0\left(x_n'\sin\theta\cos\varphi + y_n'\sin\theta\sin\varphi\right)} \int_{-h_n}^{h_n} I_n\left(z_n'\right) e^{jk_0 z_n'\cos\theta} dz_n' \right\} \tag{9}$$

Substituting $\omega\mu_0 = k_0\eta_0$ in equation 9, we have

$$E_\theta = \frac{jk_0\eta_0 e^{-jk_0 r}\sin\theta}{4\pi r}\sum_{n=1}^{N}\left\{ e^{jk_0\left(x_n'\sin\theta\cos\varphi + y_n'\sin\theta\sin\varphi\right)} \int_{-h_n}^{h_n} I_n\left(z_n'\right) e^{jk_0 z_n'\cos\theta} dz_n' \right\} \tag{10}$$

Using equation for $I_n\left(z_n'\right)$ in equation 10, this results to

$$E_\theta = \frac{jk_0\eta_0 e^{-jk_0 r}\sin\theta}{4\pi r}\sum_{n=1}^{N}\left\{ e^{jk_0\left(x_n'\sin\theta\cos\varphi + y_n'\sin\theta\sin\varphi\right)} \sum_{m=1}^{M} I_{nm} \int_{-h_n}^{h_n} \cos\left[\frac{(2m-1)\pi z_n'}{2h_n}\right] e^{jk_0 z_n'\cos\theta} dz_n' \right\} \tag{11}$$

This then becomes

$$E_\theta = \frac{jk_0\eta_0 e^{-jk_0 r}\sin\theta}{4\pi r}\sum_{n=1}^{N}\left\{ e^{jk_0\left(x_n'\sin\theta\cos\varphi + y_n'\sin\theta\sin\varphi\right)} \sum_{m=1}^{M} I_{nm} \int_{0}^{h_n} 2\cos\left[\frac{(2m-1)\pi z_n'}{2h_n}\right]\left[\frac{e^{jk_0 z_n'\cos\theta} + e^{-jk_0 z_n'\cos\theta}}{2}\right] dz_n' \right\} \tag{12}$$

`

$$\frac{e^{jk_0z_n'\cos\theta}+e^{-jk_0z_n'\cos\theta}}{2}=\frac{\cos\left(k_0z_n'\cos\theta\right)+j\sin\left(k_0z_n'\cos\theta\right)+\cos\left(k_0z_n'\cos\theta\right)-j\sin\left(k_0z_n'\cos\theta\right)}{2}$$

13)

$$\frac{e^{jk_0z_n'\cos\theta}+e^{-jk_0z_n'\cos\theta}}{2}=\cos\left(k_0z_n'\cos\theta\right) \quad (14)$$

Using equation 14 in equation 12, we have

$$E_\theta=\frac{jk_0\eta_0e^{-jk_0r}\sin\theta}{4\pi r}\sum_{n=1}^{N}\left\{e^{jk_0\left(x_n'\sin\theta\cos\varphi+y_n'\sin\theta\sin\varphi\right)}\sum_{m=1}^{M}I_{nm}\int_0^{h_n}2\cos\left[\frac{(2m-1)\pi z_n'}{2h_n}\right]\cos\left(k_0z_n'\cos\theta\right)dz_n'\right\} \quad (15)$$

Since

$$\int\cos ax\cos bxdx=\frac{\sin(a+b)x}{2(a+b)}+\frac{\sin(a-b)x}{2(a-b)} \quad (16)$$

With the help of 16, integral part of equation 15 is obtained

$$a=\frac{(2m-1)\pi}{2h_n},b=k_0\cos\theta \quad (17)$$

$$\int_0^{h_n}2\cos\left[\frac{(2m-1)\pi z_n'}{2h_n}\right]\cos\left(k_0z_n'\cos\theta\right)=\frac{\sin\left[\left(\frac{(2m-1)\pi}{2h_n}+k_0\cos\theta\right)h_n\right]}{\left(\frac{(2m-1)\pi}{2h_n}+k_0\cos\theta\right)}+\frac{\sin\left[\left(\frac{(2m-1)\pi}{2h_n}-k_0\cos\theta\right)h_n\right]}{\left(\frac{(2m-1)\pi}{2h_n}-k_0\cos\theta\right)} \quad (18)$$

$$\int_0^{h_n}2\cos\left[\frac{(2m-1)\pi z_n'}{2h_n}\right]\cos\left(k_0z_n'\cos\theta\right)=\frac{\left[\sin\left(\frac{(2m-1)\pi}{2h_n}+k_0\cos\theta\right)h_n\right]h_n}{\left(\frac{(2m-1)\pi}{2h_n}+k_0\cos\theta\right)h_n}+\frac{\left[\sin\left(\frac{(2m-1)\pi}{2h_n}-k_0\cos\theta\right)h_n\right]h_n}{\left(\frac{(2m-1)\pi}{2h_n}-k_0\cos\theta\right)h_n} \quad (19)$$

`

$$D^{+}=\left(\frac{(2m-1)\pi}{2h_n}+k_0\cos\theta\right)h_n \tag{20}$$

and

$$D^{-}=\left(\frac{(2m-1)\pi}{2h_n}-k_0\cos\theta\right)h_n \tag{21}$$

Using equations 20 and 21 in 19, we have

$$\int_0^{h_n}2\cos\left[\frac{(2m-1)\pi z_n'}{2h_n}\right]\cos\left(k_0 z_n'\cos\theta\right)=\left[\frac{\sin\left(D^{+}\right)}{D^{+}}+\frac{\sin\left(D^{-}\right)}{D^{-}}\right]h_n \tag{22}$$

Substituting equation 22 in equation 15, we have

$$E_\theta=\frac{jk_0\eta_0 e^{-jk_0r}\sin\theta}{4\pi r}\sum_{n=1}^{N}\left\{e^{jk_0\left(x_n'\sin\theta\cos\varphi+y_n'\sin\theta\sin\varphi\right)}\sum_{m=1}^{M}I_{nm}\left[\frac{\sin\left(D^{+}\right)}{D^{+}}+\frac{\sin\left(D^{-}\right)}{D^{-}}\right]\right\}h_n \tag{23}$$

The Electric field $\bar{E}$ and magnetic field $\bar{H}$ are interdependent. Therefore the associated magnetic field is

$$H_\varphi=\frac{E_\theta}{\eta_0} \tag{24}$$

$$H_\varphi=\frac{jk_0 e^{-jk_0r}\sin\theta}{4\pi r}\sum_{n=1}^{N}\left\{e^{jk_0\left(x_n'\sin\theta\cos\varphi+y_n'\sin\theta\sin\varphi\right)}\sum_{m=1}^{M}I_{nm}\left[\frac{\sin\left(D^{+}\right)}{D^{+}}+\frac{\sin\left(D^{-}\right)}{D^{-}}\right]\right\}h_n \tag{25}$$

`

Appendix D

```
%  Electric and magnetic fields of Yagi uda antennas for Direction
%  Finding System respectively, for N equals 5

k=1;% k=wave number
 r=50;% distance from antenna to far field

curr= curre;% curre=current through the dipole
imp=377;% intrinsic impedance
pi=3.142;% 22/7

    sumf1=zeros(1,300);
     sumf2=zeros(1,300);
```

```
`
    sumle=zeros(1,300);
    elefield=zeros(1,300);
    magfield=zeros(1,300);
    sn1=zeros(1,300);
    b=zeros(1,300);

leng(1)=0.25;
leng(2)=0.22;
leng(3)=0.211;
leng(4)=0.202;
leng(5)=0.193;
dist(1)=0;
dist(2)= 0.108;
dist(3)= 0.086;
dist(4)= 0.069;
dist(5)= 0.052;

    angle1=0.01:0.01:0.01*size(b,2);
 for sn1=1:1:300;
    b(sn1)=cos(angle1(sn1));
            sumf1=0;


         for leng=1:1:5;
```

```
`
            field1=(cos(k*leng*cos (angle1(sn1)))-(cos(k*leng))).(sin
(angle1(sn1)));
            sumf1=sumf1+field1;

          end
          sumf2=0;
          for dist=1:1:5;

             fx1=exp((1i)*k*dist.*cos(angle1(sn1)));
             sumf2=sumf2+fx1;

          end

         sumle(sn1)=sumf1.*sumf2;

     elefield=(((1i)*imp*curr*exp(-(1i)*k*r))./(2*pi*r)).*sumle;

  end;

  for sn1=1:1:300;
    b(sn1)=cos(angle1(sn1));
            sumf1=0;


          for leng=1:1:5;
```

```
`
            field1=(cos(k*leng*cos (angle1(sn1)))-(cos(k*leng))./(sin
(angle1(sn1)));
            sumf1=sumf1+field1;

          end
          sumf2=0;
          for dist=1:1:5;

            fx1=exp((1i)*k*dist.*cos(angle1(sn1)));
            sumf2=sumf2+fx1;

          end

         sumle(sn1)=sumf1.*sumf2;

    magfield=(((1i)*curr*exp(-(1i)*k*r))./(2*pi*r)).*sumle;
     end;
subplot (1,2,1);
polar(angle1,abs(elefield));
 xlabel('E Field');
subplot (1,2,2);
polar(angle1,abs(magfield));
 xlabel('H Field');
```

`

Appendix E

```
%  avepoynting of Yagi uda antennas for Direction Finding System, for N equals 5

k=1; % k=wave number
 r=50;% distance from antenna to far field

curr= curre; % curre=current through the dipole
imp=377;% intrinsic impedance
pi=3.142;% 22/7
```

`

```
    sumf1=zeros(1,300);
    sumf2=zeros(1,300);
    sumlepoynting=zeros(1,300);
    avepoynting=zeros(1,300);
    sn1=zeros(1,300);
    b=zeros(1,300);

leng(1)=0.25;
leng(2)=0.22;
leng(3)=0.211;
leng(4)=0.202;
leng(5)=0.193;
dist(1)=0;
dist(2)= 0.108;
dist(3)= 0.086;
dist(4)= 0.069;
dist(5)= 0.052;

      angle1=0.01:0.01:0.01*size(b,2);
 for sn1=1:1:300;
    b(sn1)=cos(angle1(sn1));
            sumf1=0;

         for leng=1:1:5;
```

```
`
            field1=(cos(k*leng*cos (angle1(sn1)))-(cos(k*leng))./(sin
(angle1(sn1)));
            sumf1=sumf1+field1;
          end
          sumf2=0;
          for dist=1:1:5;
             fx1=exp((1i)*k*dist.*cos(angle1(sn1)));
            sumf2=sumf2+fx1;
          end
          sumlepoynting(sn1)=(sumf1.*sumf2).^2;

     avepoynting=(((1i)*imp*curr*exp(-
(1i)*k*r))./(8*pi^2*r^2)).*sumlepoynting;
   end;
polar(angle1,abs(avepoynting));
 xlabel(' Average poynting Vector ');
```

Appendix F

```
%  radiationintensity of Yagi uda antennas for Direction
%  Finding System, for N equals 5

k=1;% k=wave number
r=50;% distance from antenna to far field
 curr= curre;% curre=current through the dipole
imp=377;% intrinsic impedance
pi=3.142;% 22/7
```

`

```
 sumf1=zeros(1,300);
sumf2=zeros(1,300);
sumlepoynting=zeros(1,300);
radiationintensity=zeros(1,300);
sn1=zeros(1,300);
b=zeros(1,300);

leng(1)=0.25;
leng(2)=0.22;
leng(3)=0.211;
leng(4)=0.202;
leng(5)=0.193;
dist(1)=0;
dist(2)= 0.108;
dist(3)= 0.086;
dist(4)= 0.069;
dist(5)= 0.052;
 angle1=0.01:0.01:0.01*size(b,2);
 for sn1=1:1:300;
    b(sn1)=cos(angle1(sn1));
          sumf1=0;

       for leng=1:1:5;
```

```
`
            field1=(cos(k*leng*cos (angle1(sn1)))-(cos(k*leng))./(sin
(angle1(sn1)));
            sumf1=sumf1+field1;
          end
          sumf2=0;
          for dist=1:1:5;

            fx1=exp((1i)*k*dist.*cos(angle1(sn1)));
            sumf2=sumf2+fx1;
          end

         sumlepoynting(sn1)=(sumf1.*sumf2).^2;

     radiationintensity=(((1i)*imp*curr*exp(-
(1i)*k*r))./(8*pi^2)).*sumlepoynting;

  end;
polar(angle1,abs(radiationintensity));
 xlabel('radiation intensity');
```

`

Appendix G

```
%  Directivity of dipole antenna for Direction
%  Finding System

 x=0:0.1: pi;

directivity=1.5.*sin(x);
```

`

```
size (x);
size (dd);

polar(x,abs(directivity))
xlabel ('theta')
ylabel ('Directivity')
title ('Directivity of a Dipole')
```

Appendix H

```
%  Directivity of Yagi uda antennas for Direction
%  Finding System

clc
close all hidden

disp ('')
```

```
`
disp ('press any key to enter the distance d in meter between elements')
pause
d= input ('enter the distance d in meter between elements');
k=2*pi/lambda;
theta=0:0.01:pi;
psi=(k*d*cos(theta));

 f=input('please enter the operating frequency in Hz:\n?');
N=input('please enter the no of element (N):\n?');

lambda=(3*(10^8))/f; %lambda=c/f%the value in meter;

z1=(N/2)*(psi);
z2=(1/2)*(psi);
AF=sin(z1)./(sin(z2));
w=abs(AF);

directivity=1.5.*sin(theta).*w;

size (theta);
size (directivity);

polar(theta,abs(directivity))

xlabel ('Directivity of yagi array')
```

`

disp(directivity)

Appendix I

% Directive Gain of dipole antenna for Direction

% Finding System

k=1;% k=wave number

imp=377;% intrinsic impedance

`

```
pi=3.142;% 22/7

 angle1=0:0.1:3.2;
x=(1.5).*((sin(angle1)).^2);

plot(angle1,abs(x));
 xlabel('Directive Gain');
```

Appendix J

```
%  Directive Gain of Yagi uda antennas for Direction
%  Finding System

clc
close all hidden
```

```
`
disp ('')
disp ('press any key to enter the distance d in meter between elements')
pause
d= input ('enter the distance d in meter between elements');
k=2*pi/lambda;
theta=0:0.01:pi;
psi=(k*d*cos(theta));

 f=input('please enter the operating frequency in Hz:\n?');
N=input('please enter the no of element (N):\n?');

lambda=(3*(10^8))/f; %lambda=c/f%the value in meter;

z1=(N/2)*(psi);
z2=(1/2)*(psi);
AF=sin(z1)./(sin(z2));
w=abs(AF);
 directivegain=(1.5).*((sin(theta)).^2).*w;
 polar(theta,abs(directivegain));
 xlabel('Directive Gain of the yagi array');
disp(directivegain)
```